European Journal of Medicinal Chemistry Reports 17 (2026) 100360

Contents lists available at ScienceDirect

European Journal of Medicinal Chemistry Reports

journal homepage: www.editorialmanager.com/ejmcr/default.aspx

New C-30 secondary and tertiary amines of betulin with selective antiproliferative activity toward hematological malignancies - Synthesis and biological evaluation

Jan Bachořík [a], Ivo Frydrych [b], Soňa Gurská [b], Štěpán Dostál [d], Jan Pokorný [a], Adam Přibylka [a], Martina Medvedíková [b], Petr Džubák [b], Marián Hajdúch [b], Milan Urban [c,*]

[a] Department of Organic Chemistry, Faculty of Science, Palacký University Olomouc, 17. listopadu 1192/12, Olomouc, 779 00, Czech Republic
[b] Laboratory of Experimental Medicine, Institute of Molecular and Translational Medicine, Faculty of Medicine and Dentistry, Palacký University and University Hospital Olomouc, Hněvotínská 1333/5, Olomouc, 779 00, Czech Republic
[c] Laboratory of Medicinal and Organic Chemistry, Institute of Molecular and Translational Medicine, Faculty of Medicine and Dentistry, Palacký University Olomouc, Hněvotínská 1333/5, Olomouc, 779 00, Czech Republic
[d] Department of Analytical Chemistry, Faculty of Science, Palacký University Olomouc, 17. listopadu 1192/12, Olomouc, 779 00, Czech Republic

ARTICLE INFO

Keywords:
Triterpenes
Betulin
Semi-synthesis
Tsuji-Trost
Amines
Cytotoxicity
Cancer

ABSTRACT

A novel synthetic approach for preparation of secondary and tertiary amine derivatives of betulin was developed. The synthesis starts from commercially available betulin diacetate (**1**). The final step of the sequence relied on a Tsuji–Trost reaction. To explore the scope of this procedure, we prepared a variety of substituted secondary and tertiary amines. The reaction successfully afforded 31 out of 32 target products, with only one example failing to react.

All the prepared compounds were tested for *in vitro* cytotoxic activity against 6 cancer cell lines and 2 non-cancer cell lines. Several derivatives exhibited pronounced and selective antiproliferative activity toward hematological malignancies, with compounds **5q**, **5s**, and **5t** showing the most potent effects in CCRF-CEM and K562 cells while maintaining favorable selectivity over non-cancer fibroblasts. Mechanistic studies revealed that these compounds induce replication stress, leading to S-phase cell-cycle arrest and suppression of DNA synthesis. This was accompanied by activation of DNA damage response signaling, as indicated by increased γH2AX levels and upregulation of Cyclin E1 and p21. Further analysis demonstrated involvement of the intrinsic apoptotic pathway, as evidenced by mitochondrial membrane depolarization and increased expression of the pro-apoptotic protein BAX. In contrast, limited caspase activation and minimal PARP cleavage at equitoxic concentrations indicate that cells predominantly undergo early apoptotic commitment rather than full apoptotic execution. Collectively, these findings identify replication stress-mediated cell death as a key mechanism of action and highlight aminoderivatives of betulin diacetate as promising candidates for targeting proliferation-associated vulnerabilities in leukemia cells.

1. Introduction

A recent review article highlighted the growing importance of plant extracts containing bioactive natural compounds (including terpenoids) and their role in the development of modern therapeutics useful in the treatment of the most prevalent diseases such as cancer, diabetes, and neurodegenerative disorders [1]. Acknowledging the irreplaceable role of natural products in medicinal research, our team is focused on optimizing biologically active triterpenoids, with a particular emphasis on naturally occurring betulin, to enhance their potential as medicinal agents. This molecule gained our attention because of its high availability from birch bark [2–7] and a diverse range of biological activities such as anti-cancer [8–12], anti-HIV [13,14], anti-inflammatory [10, 15], and many others [16,17]. The potentially wide-spread use of betulin is currently limited in the medicinal practice because of its hydrophobic structure which is usually responsible for low availability in per oral administration in *in vivo* experiments [18]. This issue can be addressed by targeted chemical modification that allows for enhancing

* Corresponding author.
E-mail address: milan.urban@upol.cz (M. Urban).

https://doi.org/10.1016/j.ejmcr.2026.100360
Received 24 July 2026; Accepted 24 July 2026
Available online 28 July 2026

bioavailability while retaining or enhancing the biological activity, sometimes preventing undesirable side-effects [19]. Betulin structure offers three main sites for the chemical functionalization - positions C-3, C-28 [14,20–36], and somewhat less investigated position C-30 [30, 37–53]. To our surprise, only a small number of publications were dedicated to the use of amine modifications at the position C-30 [41–44], although it has been recognized by the scientific community that amine moiety is capable of a significant decrease in lipophilicity of hydrophobic compounds while retaining the original biological activity [54]. Similarly to betulin, amine derivatives of betulinic acid are rather unexplored. A recent example of such a study is a publication from 2025 [55].

Inspired by earlier work [43,44,55] and encouraged by an urgent need for biologically active triterpenoids with superior solubility in polar media to existing compounds, we decided to develop a new, robust and efficient synthetic approach while avoiding the formerly used reaction scheme using NBS/CCl_4 for the introduction of bromine to the molecule that then may be substituted with amines [43,44,55]. Especially since CCl_4 is being gradually phased out due to health and environmental concerns [56]. The proposed synthetic strategy is based on our previous success with the improved introduction of hydroxy group to the position C-30 in two steps [57]. The hydroxy derivative can undergo the Tsuji-Trost replacement under appropriate conditions [58]. Alternatively, acetylation of the hydroxy group may facilitate this reaction, enabling the introduction of secondary or tertiary groups at the position C-30 [59]. To the best of our knowledge, the only previous amination at the position C-30 of lupane triterpenoids was described by Evers et al. who modified betulinic acid analogues, however, this approach has never been used in the chemistry of betulin or betulin diacetate (**1**) [60]. In our most recent study [57], we prepared three aniline derivatives of betulin diacetate and one phthalimide derivative utilizing a Mitsunobu protocol. Nevertheless, because this procedure required amine protection with Ts- or Ns-protecting groups, the development of a more elegant and general method was highly desirable. Herein, a comprehensive library of 31 amine derivatives was synthesized using this novel approach and subsequently evaluated for cytotoxic activity.

2. Results and discussion

2.1. Chemistry

Initially, hydroxy derivative **3** was prepared from betulin diacetate (**1**) using our previously published protocol [57]. This was followed by acetylation of free hydroxy group (Scheme 1). We aimed to evaluate both compounds as substrates for the final Tsuji-Trost reaction to determine which one would be more suitable.

Following the successful preparation of both substrates **3** and **4**, our attention was directed towards their coupling with a range of primary and secondary amines under Pd(0) catalysis. The palladium catalyst was generated from $Pd(OAc)_2$ and Tris(3-sulfophenyl)phosphine trisodium salt ligand (TPPTS). These reagents were deliberately chosen because of their superior solubility in water, which offers a simplified work-up procedure. The second reason was attributed to previously reported high yields [58]. Building on these findings concerning $Pd(OAc)_2$ and TPPTS, we developed an optimized protocol specifically tailored for our compounds. Based on our previous experience with triterpenoid chemistry, we specifically designed the solvent system and reagent stoichiometry to ensure compatibility and to maximize yields. The modified protocol employed a THF/H_2O solvent system instead of original EtOAc/H_2O, excess of amine and utilized ester **4** as the substrate in place of compound **3**, as no reaction was observed in our initial attempt with the latter. The hydroxy group of the compound **3** was found to be inferior in reactivity compared to the acetoxy group under our experimental conditions. Initially, the feasibility of the reaction was demonstrated by the preparation of compound **5a** bearing aliphatic substituent in high yield (Scheme 2). Subsequently, deliberately designed molecules (**5b-e**) were synthesized to evaluate the scope of the protocol, especially for the preparation of more complex derivatives containing several common functional groups. Rather low yield of **5c** was probably caused by the electron-withdrawing effect of the proximal ester function to amine group. To investigate the reaction scope further, we focused on the preparation of secondary amines containing either unsubstituted or substituted aromatic moieties, as well as heterocycles. These substituents were selected to include standard electron-donating and electron-withdrawing functionalities in order to be able to evaluate their effect on reactivity and stability under the given conditions.

Furthermore, this selection was guided by our preliminary biological data indicating promising activity (discussed in biological section). The reaction proved to be tolerant in all tested cases, though yields were generally higher with electron-donating groups. For aniline-substituted compound **5y**, no reaction occurred even after 48 h, proving the Tsuji–Trost protocol unsuitable for this specific class of derivatives. However, we previously established that the Mitsunobu protocol is effective in this case, albeit requiring additional protection/deprotection steps [57]. To further demonstrate the synthetic versatility of the protocol, selected examples **6a** and **6b** containing tertiary amine groups were successfully synthetized. Both compounds were prepared in high yields (90% and 82%). Preparation of a broader set of structurally similar compounds was not pursued due to negligible activity in preliminary cytotoxic screening. To expand the scope of reaction further, tertiary amines with cyclic amine moieties were also synthetized. All compounds were prepared with yields exceeding 70%. Amine **7e** with protected piperazine linker was prepared as a proof-of-concept which could be further utilized in preparation of more intricate molecules in the future.

The acetyl groups at the position C-3 and C-28 of the terpenoid skeleton were not removed at the end since the activity of several compounds in this study was high and we know from the previous work [61,62], that the presence of more than two hydrogen bond donors around the triterpenoid molecule usually leads to low solubility in both polar and lipophilic solvents.

2.2. Biology

2.2.1. Cytotoxic response profiles across cancer and non-cancer Cell models

The cytotoxicity assessment across a broad panel of hematological and solid tumor cell lines revealed a clear stratification in the biological activity of the tested nitrogen-based derivatives **5a** – **7e** as well as the starting compounds and intermediate **1**–**4** (Table 1). While a substantial portion of compounds exhibited limited or no cytotoxicity

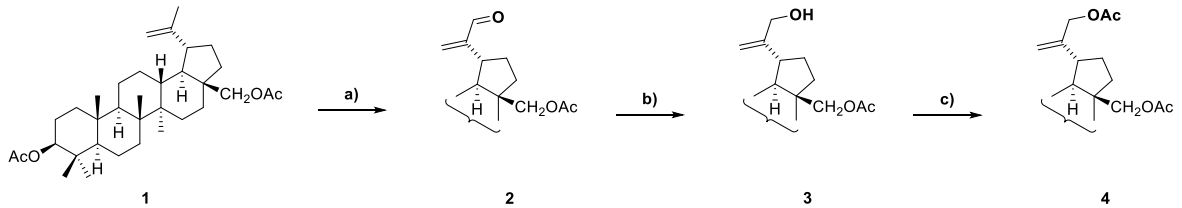

Scheme 1. Reagents and conditions: **a)** SeO_2, TBHP, DCM, AcOH, rt, 48 h; 84% **b)** $NaBH_4$, $CeCl_3 \cdot 7H_2O$, THF, MeOH, 15 min, 78%; **c)** Ac_2O, Py, 24 h, 95%.

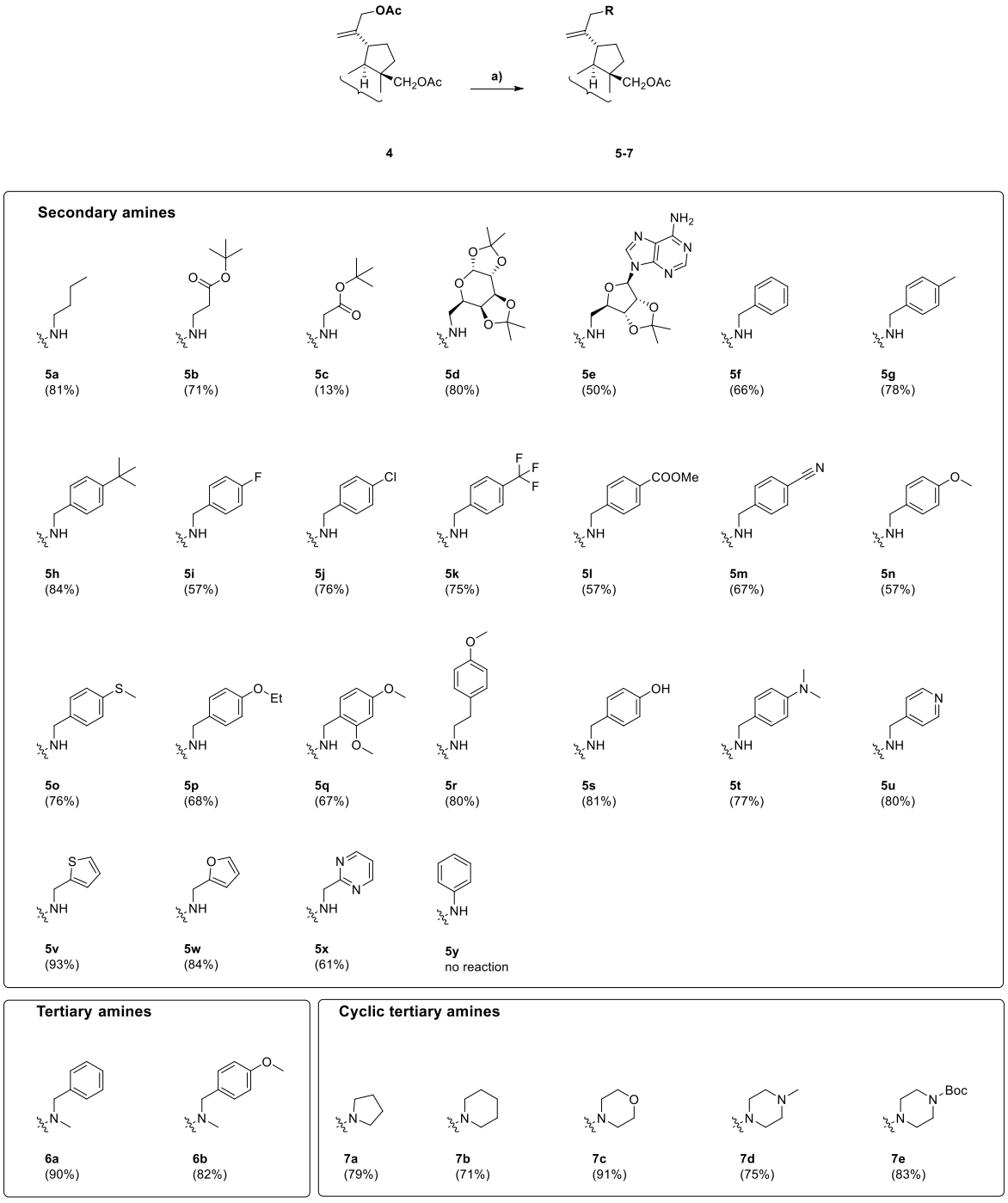

Scheme 2. Reagents and conditions: primary amine or secondary amine, $Pd(OAc)_2$, TPPTS, K_2CO_3, THF, H_2O, 60 °C, 24–48 h.

($IC_{50} > 50$ μM), a distinct cluster showed pronounced and often highly selective antiproliferative effects. The most striking activities were consistently observed in the CCRF-CEM leukemia model, which emerged as the most responsive system in the entire dataset, allowing the identification of a series of structurally related molecules with low-micromolar inhibitory potency. Among these, aldehyde **2** and amines **5q**, **5s**, and **5t** were selected for subsequent detailed biological evaluation because they demonstrated the most potent and uniform activity profiles. All four showed IC_{50} values within the low-micromolar or even submicromolar range in CCRF-CEM, accompanied by comparably strong effects in K562 and moderate activity across selected solid tumor lines. At the same time, their IC_{50} values in non-cancer fibroblasts (BJ, MRC-5) remained slightly higher, yielding a therapeutically narrower selectivity window providing a valuable baseline for further structural optimization. Beyond the primary hits, several additional compounds displayed highly notable and biologically informative activity patterns. A small group of derivatives, including **5d**, **5g**, **5i**, and **5p**, showed a selective cytotoxic preference for hematological cancer models, combining low-micromolar activity in CCRF-CEM with similarly potent effects in K562 while remaining largely inactive toward fibroblasts and most solid tumor lines. This selective responsiveness suggests that these molecules target leukemia-specific molecular pathways or signaling nodes conserved across acute and chronic myeloid malignancies. Particularly intriguing is the behavior of **5f**, which stands out as a uniquely selective cytotoxic agent for the K562 chronic myeloid leukemia model. Unlike most compounds active in K562, **5f** exhibits no measurable cytotoxicity

Table 1
Cytotoxicity (IC_{50}, μmol/L) of library compounds tested on six cancer cell lines (CCRF-CEM, HCT116, HCT116p53−/−, K562, A549, U2OS) and two non-cancerous cell lines (BJ, MRC-5).

Compound	IC_{50} (μmol/L)[a]								
	CCRF-CEM	HCT116	HCT116p53-	K562	A549	U2OS	BJ	MRC-5	SI[b]
1	>50	>50	>50	>50	>50	>50	>50	>50	-
2	0.96	1.5	1.5	1.6	16	1.5	1.8	2.9	2.4
3	18	31	35	25	32	23	>50	>50	>2.8
4	>50	>50	>50	>50	>50	>50	>50	>50	-
5a	4.7	6.9	6.9	6.2	6.5	6.3	6.2	6.6	1.4
5b	9.1	28	27	10	31	25	28	27	3.0
5c	>50	>50	>50	>50	>50	>50	>50	>50	-
5d	7.8	19	21	8.3	>50	22	33	31	4.1
5e	12	>50	>50	32.19	>50	>50	>50	>50	>4.2
5f	>50	45	40	12	>50	47	>50	>50	-
5g	14	31	35	6.8	>50	33	>50	33	>3.0
5h	46	>50	>50	>50	>50	>50	>50	>50	>1.1
5i	21	>50	>50	12	>50	>50	>50	>50	>2.4
5j	>50	>50	>50	>50	>50	>50	>50	>50	-
5k	23	>50	>50	>50	>50	>50	>50	>50	>2.2
5l	23	>50	>50	24.3	>50	>50	>50	>50	>2.2
5m	>50	>50	>50	>50	>50	>50	>50	>50	-
5n	5.9	9.8	10	3.6	24	8.5	13	26	3.2
5o	11	40	>50	4.7	>50	34	26	42	3.0
5p	8.4	28	27	9.8	>50	26	>50	>50	>5.9
5q	3.9	7	7.1	3.1	6.3	6.1	6.5	6.5	1.7
5r	4.9	6.8	6.9	5.7	8.2	6.4	6.4	6.7	1.3
5s	3.7	6.7	7.2	4.0	6.4	6.6	6.4	6.6	1.7
5t	2.7	6.4	7.2	2.3	6.2	6.3	7.0	6.8	2.5
5u	12	18	20	15	26	15	20	12	1.3
5v	30	>50	>50	>50	>50	>50	>50	>50	>1.7
5w	19	>50	>50	26	>50	>50	>50	>50	>2.7
5x	11	25	29	11	27	24	26	27	2.3
6a	>50	>50	>50	>50	>50	>50	>50	>50	-
6b	>50	>50	>50	>50	>50	>50	>50	>50	-
7a	11.5	30	31	11	33	26	31	25	2.5
7b	22	>50	>50	>50	>50	>50	>50	>50	>2.2
7c	30	>50	>50	>50	>50	>50	>50	>50	>1.7
7d	4.4	9.6	11	6.1	17	6.	20	8.6	3.3
7e	>50	>50	>50	>50	>50	>50	>50	>50	-

[a] The IC_{50} represents the concentration of the drug required to inhibit cell growth by 50%. The standard deviation in cytotoxicity assays typically reaches up to 15% of the mean value. Full table with standard deviations is in the SI file.
[b] The selectivity index is calculated based on the IC_{50} for the CCRF-CEM line versus the average IC_{50} for both fibroblast lines.

toward CCRF-CEM, despite the latter being the most sensitive line in the entire panel, nor toward any solid tumor model. Its activity is thus sharply confined to a single hematological lineage. Such narrow selectivity is rare within the dataset and suggests a biological target or vulnerability specific to the BCR-ABL - positive phenotype characteristic of K562 cells. The divergence between its inactivity in CCRF-CEM (ALL lineage) and pronounced activity in K562 (CML lineage) raises the possibility that **5f** interacts with pathways modulated by the Philadelphia chromosome or downstream signaling processes essential for BCR-ABL driven proliferation which warrants future studies of this mechanism of action. Compounds with such lineage-restricted effects are valuable chemical probes and could offer insights into CML-specific biochemical dependencies. Collectively, the dataset reveals two principal mechanistic and SAR-relevant patterns. First, a cluster of broadly active leukemia-targeting compounds, including the lead molecules **2**, **5q**, **5s** and **5t**, as well as the secondary hits **5d**, **5g**, **5i**, and **5p,** demonstrate consistent low-micromolar potency across CCRF-CEM and K562. This suggests that these derivatives share a pharmacophore capable of targeting cellular processes commonly dysregulated across hematological malignancies. Second, the unique behavior of **5f** points to the existence of structurally encoded selectivity determinants capable of discriminating between individual leukemia subtypes based on their molecular pathogenesis.

2.2.2. *Induction of apoptotic Cell death in CCRF-CEM cells*

Based on the cytotoxicity profiling described above (Section 2.2.1), compounds **2**, **5q**, **5s**, and **5t**, which displayed the most potent antiproliferative activity and the most favorable selectivity indices toward the CCRF-CEM leukemia model, were further evaluated for their ability to induce cell death and its underlying mode. To this end, apoptotic and necrotic cell populations were quantitatively assessed using Annexin V/propidium iodide (PI) dual staining followed by flow-cytometric analysis (Fig. 1). Treatment of CCRF-CEM cells with all four selected compounds resulted in a clear, concentration-dependent induction of apoptotic cell death. At concentrations corresponding to 1 × IC_{50}, the predominant cell population remained Annexin V/PI double-negative, indicating that early cytotoxic effects at this exposure level are not associated with extensive plasma membrane compromise. Nevertheless, a reproducible increase in Annexin V-positive/PI-negative cells was already evident, particularly for compounds **2**. At higher concentrations (5 × IC_{50}), all four derivatives triggered a pronounced shift toward late apoptotic and apoptotic/secondary necrotic cell populations, as reflected by a substantial increase in Annexin V/PI double-positive cells. Under these conditions, the percentage of viable cells dropped dramatically, accompanied by a marked accumulation of fragmented and membrane-compromised cells. This effect was most prominent for compounds **5q**, **5s**, and **5t**, all of which induced extensive apoptotic cell death exceeding 50% of the total population, whereas compound **2** displayed a somewhat attenuated, yet still significant, response. The minimal fraction of PI-positive/Annexin V-negative cells across all treatments indicates that primary necrosis is not a dominant mode of cell death and that apoptosis represents the principal mechanism underlying compound-induced cytotoxicity. Importantly, the apoptotic profiles observed by Annexin V/PI staining are in good

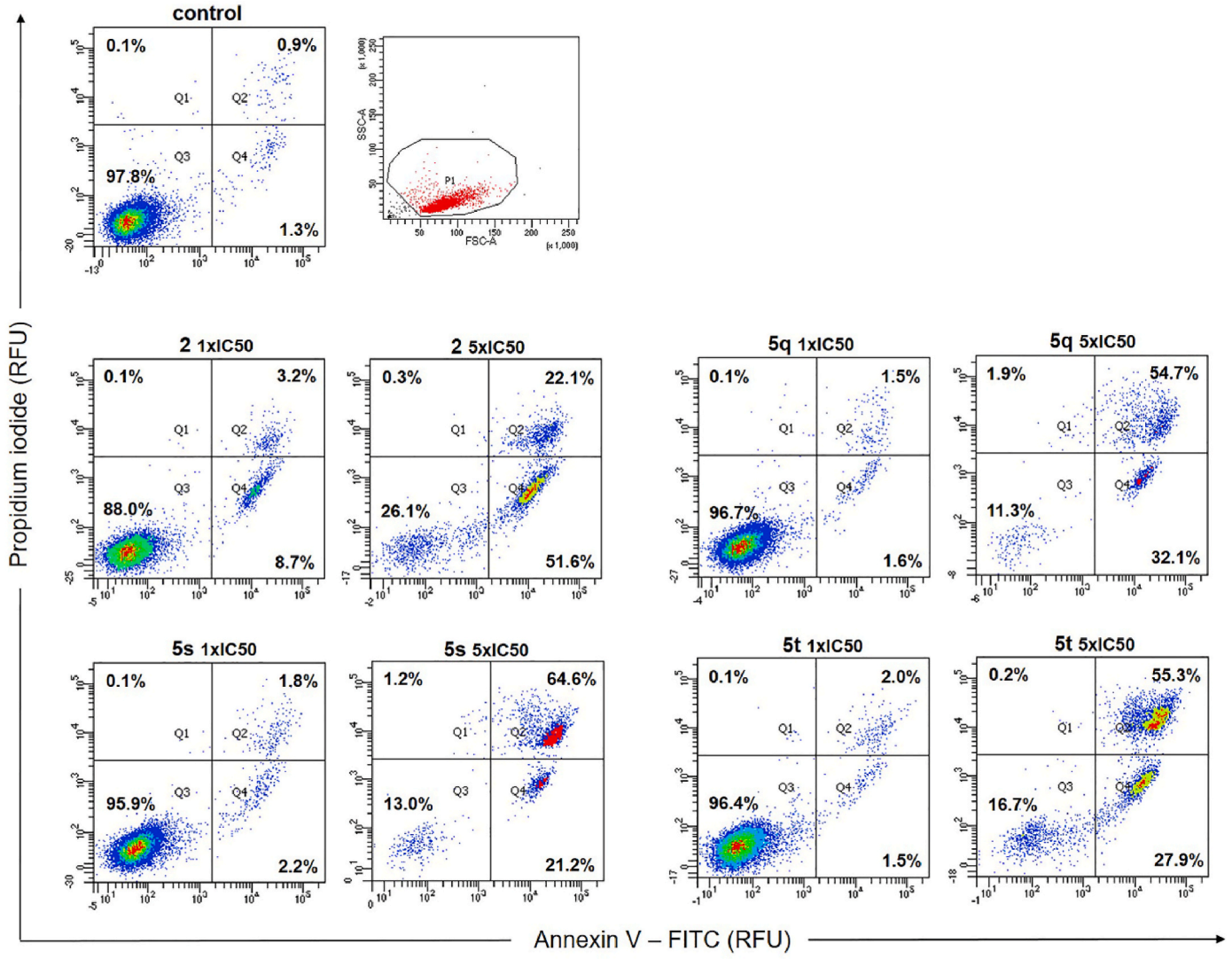

Fig. 1. Induction of apoptotic cell death in CCRF-CEM cells treated with selected compounds. Apoptotic cell death in CCRF-CEM leukemia cells was analyzed by flow cytometry using Annexin V-FITC and propidium iodide (PI) double staining following treatment with compounds **2**, **5q**, **5s**, and **5t** at concentrations corresponding to 1 × and 5 × IC_{50}. A forward scatter (FSC) versus side scatter (SSC) dot plot is shown in the upper right panel, illustrating the gating strategy used for analysis; gate P1 was applied to exclude cell debris and aggregates and to select the main population of intact single cells for further evaluation. Representative Annexin V/PI dot plots of gated cells show the distribution of viable cells (Annexin V^-/PI^-, lower left quadrant), early apoptotic cells (Annexin V^+/PI^-, lower right quadrant), and late apoptotic or apoptotic/secondary necrotic cells (Annexin V^+/PI^+, upper right quadrant).

agreement with the antiproliferative effects determined in the MTS [3-(4,5-dimethylthiazol-2-yl)-5-(3-carboxymethoxyphenyl)-2-(4-sulfophenyl)-2H-tetrazolium] assay, reinforcing the conclusion that growth inhibition in CCRF-CEM cells reflects active induction of programmed cell death rather than nonspecific cytotoxic damage. The gradual transition from early to late apoptotic populations with increasing compound concentration further suggests a regulated death process rather than an acute loss of cellular integrity. These findings provide functional evidence that the strong cytotoxicity of compounds **2**, **5q**, **5s**, and **5t** toward leukemia cells is mechanistically coupled to apoptosis induction. The concentration-dependent nature of the apoptotic response, together with the limited necrotic contribution, strongly implies engagement of intrinsic cellular death pathways rather than catastrophic membrane disruption. This observation is particularly relevant in light of the favorable therapeutic window observed for these compounds, as apoptosis-driven cytotoxicity is generally associated with improved selectivity and reduced inflammatory side effects. On this basis, subsequent experiments were aimed at elucidating whether apoptotic signaling is linked to mitochondrial dysfunction and to identify the primary cellular events that precede the onset of cell death.

2.2.3. Mitochondrial membrane depolarization during compound-induced Cell death

Given the pronounced induction of apoptotic cell death observed after 24 h of treatment by Annexin V/PI staining (Section 2.2.2), we next examined whether compound-induced apoptosis is associated with mitochondrial dysfunction, a key hallmark of the intrinsic apoptotic pathway (Fig. 2). Changes in mitochondrial transmembrane potential (ΔΨm) were therefore assessed by flow-cytometric analysis using the JC-1 fluorescent probe. Initial experiments employing a 24 h treatment interval revealed that exposure of CCRF-CEM cells to higher compound concentrations (5 × IC_{50}) resulted in extensive cellular destruction, characterized by a near-complete loss of intact cells within the FSC/SSC gate (P1) used for ΔΨm evaluation. Under these conditions, the remaining events consisted predominantly of debris and fragmented material, rendering reliable assessment of mitochondrial membrane potential impossible. Consequently, the treatment interval was shortened to 6 h for all JC-1 experiments, allowing analysis of mitochondrial

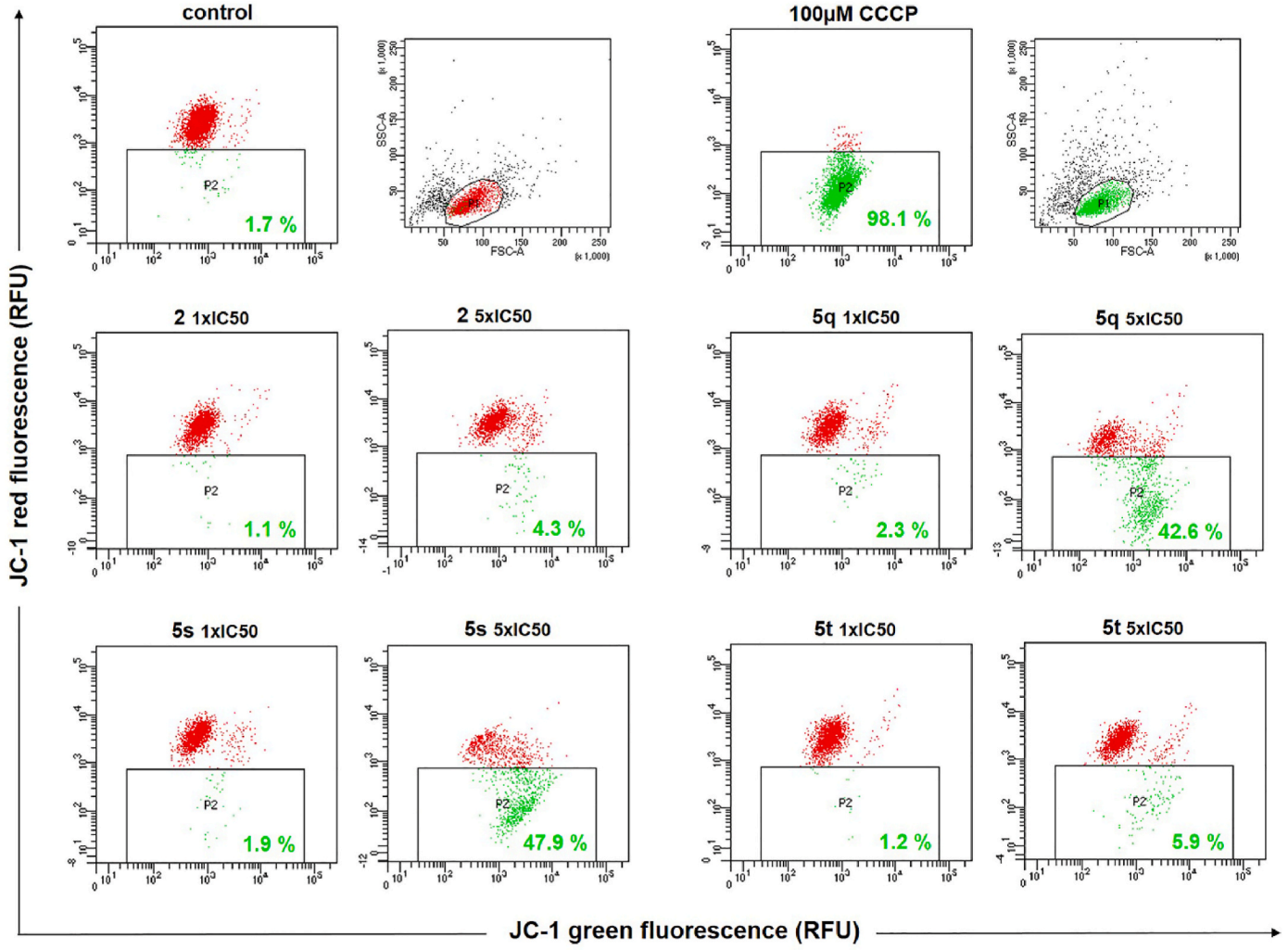

Fig. 2. Mitochondrial membrane depolarization induced by selected compounds in CCRF-CEM cells. Mitochondrial transmembrane potential (ΔΨm) in CCRF-CEM cells was assessed by flow cytometry using the JC-1 fluorescent probe following treatment with compounds **2**, **5q**, **5s**, and **5t** at concentrations corresponding to 1 × and 5 × IC_{50} for 6 h. A forward scatter (FSC) versus side scatter (SSC) dot plot (upper right panels) illustrates the gating strategy applied prior to ΔΨm analysis; gate P1 was used to select the main population of intact cells and to exclude cell debris and fragmented events, which predominated at longer treatment times or higher cytotoxic burden. Only cells within gate P1 were included in the JC-1 analysis. Representative JC-1 dot plots of gated cell populations are shown, with red fluorescence corresponding to JC-1 aggregates in mitochondria with intact membrane potential and green fluorescence indicating JC-1 monomers in depolarized mitochondria. The percentage of cells exhibiting loss of mitochondrial membrane potential (JC-1 green-positive population, gate P2) is indicated in each panel. Untreated control cells displayed predominantly polarized mitochondria with minimal ΔΨm loss, whereas treatment with the mitochondrial uncoupler CCCP (100 μM), used as a positive control, resulted in near-complete mitochondrial depolarization, validating the assay performance.

function at an earlier stage preceding irreversible cellular disintegration. All data presented in this section therefore corresponds to a 6 h treatment period. Untreated CCRF-CEM cells displayed a typical JC-1 staining pattern dominated by red fluorescence, indicative of polarized mitochondria, with only a minimal fraction of cells exhibiting green fluorescence corresponding to depolarized mitochondria. Treatment with the protonophore CCCP (100 μM), used as a positive control, resulted in an almost complete shift toward the JC-1 green-positive population, confirming the robustness and sensitivity of the assay. The clearly defined separation between polarized and depolarized mitochondrial states provided a reliable reference for evaluating compound-induced effects under sub-lethal conditions. At concentrations corresponding to 1 × IC_{50}, compounds **2**, **5q**, **5s**, and **5t** induced only minimal mitochondrial depolarization after 6 h of treatment, with the majority of cells retaining intact ΔΨm. This finding indicates that early cytotoxic or growth-inhibitory effects are not immediately associated with mitochondrial collapse. In contrast, exposure to higher concentrations (5 × IC_{50}) resulted in a pronounced, compound-dependent dissipation of mitochondrial membrane potential. Compounds **5q** and **5s** elicited the most prominent effects, with nearly half of the gated cell population exhibiting loss of ΔΨm, whereas compound **5t** induced a more moderate but clearly detectable depolarization. In line with its weaker apoptotic phenotype, compound **2** caused only limited mitochondrial depolarization even at elevated concentrations. Notably, the ΔΨm loss observed at 6 h precedes the extensive Annexin V/PI-positive late apoptotic populations detected after 24 h of treatment, indicating that mitochondrial dysfunction represents an early and critical checkpoint event during compound-induced apoptosis. The concentration dependence of mitochondrial depolarization closely mirrors the apoptotic patterns observed in the previous section, supporting a mechanistic link between ΔΨm dissipation and execution of programmed cell death. Differences in the magnitude of mitochondrial effects among individual compounds further suggest that, while all four derivatives engage the intrinsic apoptotic pathway, they may do so with differing efficiencies or kinetic profiles. Collectively, these results demonstrate that the potent cytotoxicity of compounds **2**, **5q**, **5s**, and **5t** toward CCRF-CEM cells is

associated with early disruption of mitochondrial function, consistent with activation of the intrinsic apoptotic cascade. Importantly, the absence of substantial mitochondrial depolarization at equitoxic concentrations and early time points implies that mitochondrial damage is not the primary initiating event but rather a downstream consequence of upstream cellular stress. This observation prompted subsequent investigations into earlier perturbations of cell-cycle progression and macromolecular synthesis as potential primary triggers leading to mitochondrial apoptosis.

2.2.4. Effects of selected compounds on cell-cycle progression

The observation that compound-induced apoptosis is accompanied by mitochondrial membrane depolarization yet manifests predominantly at higher concentrations and later time points, prompted further investigation into upstream cellular events that might initiate this death cascade. We therefore analyzed the impact of compounds **2**, **5q**, **5s**, and **5t** on cell cycle progression in CCRF-CEM cells using propidium iodide (PI) staining followed by flow-cytometric evaluation of DNA content, complemented by analysis of mitotic entry. Treatment with all four compounds resulted in pronounced and highly reproducible alterations in cell-cycle distribution, characterized by a marked accumulation of cells in S phase. As shown in the quantitative bar-graph analysis (Fig. 3A) and corresponding DNA content histograms (Fig. 3B), exposure to both 1 × and 5 × IC_{50} led to a substantial increase in the S-phase fraction accompanied by a concomitant reduction in the G1 population. This effect was already evident at equitoxic concentrations and became progressively more pronounced at higher exposure levels, indicating a concentration-dependent disruption of normal cell cycle progression. Notably, the relative proportion of cells in the G2/M compartment remained largely unchanged across treatments, arguing against a predominant arrest at the G2/M transition. The S-phase accumulation was consistently observed for all four derivatives, although modest quantitative differences were apparent. Compounds **5q**, **5s**, and **5t** induced particularly strong enrichment of S-phase cells, whereas compound **2** displayed a slightly less pronounced effect. The overall shape of the PI histograms further revealed distortion and broadening of the S-phase DNA content distribution, especially at 5 × IC_{50}, suggesting perturbed DNA replication dynamics rather than synchronized progression through S phase. Such profiles are characteristic of replication stress, stalled replication forks, or impaired completion of DNA synthesis. To determine whether the observed cell cycle alterations involve perturbation of mitotic entry, the abundance of mitotic cells was independently assessed by measuring phosphorylation of histone H3 at serine 10 (pH3Ser10), a well-established marker of chromatin condensation during mitosis. As shown in Fig. 3C, treatment with the compounds investigated did not result in increased mitotic accumulation. In fact, the fraction of pH3-positive cells remained low or was further reduced at 5 × IC_{50} compared with control cells, demonstrating that the compounds do not induce a mitotic block. These results clearly exclude inhibition of mitotic progression as a primary mechanism of action and instead support the conclusion that cell cycle disruption occurs upstream of mitosis. Taken together, the combined PI-based cell cycle analysis and pH3Ser10 profiling establish S-phase perturbation as the dominant cell cycle effect of compounds **2**, **5q**, **5s**, and **5t** in CCRF-CEM cells. Importantly, the absence of mitotic accumulation, coupled with the strong S-phase enrichment and distorted DNA content profiles, points to interference with DNA replication rather than checkpoint arrest at later stages of the cell cycle. This interpretation is fully consistent with the temporal hierarchy observed in preceding experiments, where mitochondrial depolarization and apoptotic execution occurred subsequent to earlier, non-lethal cellular stress. From a mechanistic perspective, sustained disturbance of S-phase progression is well known to activate replication stress responses, ultimately leading to DNA damage signaling, cell cycle checkpoint activation, and engagement of intrinsic apoptosis pathways. The convergence of S-phase accumulation, mitochondrial dysfunction, and delayed apoptotic commitment strongly suggests that replication-associated stress represents a primary initiating event in compound-treated CCRF-CEM cells. On this basis, subsequent experiments were designed to directly assess the effects of these compounds on DNA and RNA synthesis and to evaluate activation of DNA damage response pathways at the molecular level.

2.2.5. Effects of selected compounds on DNA and RNA synthesis

The pronounced accumulation of CCRF-CEM cells in S phase observed upon treatment with compounds **2**, **5q**, **5s**, and **5t** (Section 2.2.4), together with the absence of mitotic arrest, strongly suggested that DNA replication may represent a primary cellular target. To directly assess this possibility and to further delineate the nature of the replication-associated stress, we quantified DNA and RNA synthesis using BrdU/BrU incorporation assays following compound exposure. Analysis of DNA synthesis revealed a clear and concentration-dependent suppression of replicative activity (Fig. 4A). In untreated control cells, a substantial fraction of the population incorporated BrdU, consistent with active DNA replication in proliferating CCRF-CEM cells. Treatment with all four compounds at concentrations corresponding to 1 × IC_{50} led to a marked reduction in BrdU positive cells, indicating significant impairment of DNA synthesis already at equitoxic concentrations. Notably, exposure to 5 × IC_{50} resulted in an almost complete loss of detectable BrdU incorporation for all compounds, with residual DNA synthesis approaching background levels. These findings provide direct functional evidence that the S-phase accumulation observed in cell cycle analyses reflects profound inhibition of DNA replication rather than mere redistribution of cycling cells. In parallel, RNA synthesis was assessed to evaluate whether transcriptional activity is similarly affected (Fig. 4B). At 1 × IC_{50}, all compounds induced a measurable but less dramatic decrease in RNA synthesis compared to DNA replication, suggesting that partial transcriptional activity is initially retained despite ongoing replicative stress. However, at 5 × IC_{50}, RNA synthesis was almost completely suppressed across all treatments, with BrU-positive populations dropping to minimal levels. The near total shutdown of both DNA and RNA synthesis at higher concentrations indicates a collapse of global macromolecular biosynthesis, consistent with irreversible cellular stress preceding apoptotic commitment. Importantly, the differential sensitivity of DNA versus RNA synthesis to compound treatment provides insight into the temporal hierarchy of intracellular events. The early and pronounced inhibition of DNA replication at equitoxic concentrations aligns well with the strong S-phase enrichment detected by PI-based cell cycle analysis and supports the notion that replication stress constitutes an early and primary insult. The subsequent suppression of RNA synthesis at higher concentrations likely reflects secondary effects arising from checkpoint activation, transcriptional repression, and initiation of apoptotic signaling cascades. This interpretation is further supported by the temporal separation between early cell cycle perturbations (Section 2.2.4), intermediate mitochondrial dysfunction (Section 2.2.3), and late apoptotic execution (Section 2.2.2). Taken together, the combined DNA and RNA synthesis data firmly establish inhibition of DNA replication as a central mechanistic feature of compounds **2**, **5q**, **5s**, and **5t** in CCRF-CEM cells. The near complete abrogation of DNA synthesis at higher concentrations, followed by global transcriptional shutdown, provides a coherent functional explanation for the observed S-phase arrest, mitochondrial depolarization, and apoptosis induction. Such a sequence of events is characteristic of severe replication stress leading to activation of DNA damage response pathways and engagement of intrinsic apoptotic mechanisms. Based on these findings, subsequent experiments were directed toward molecular validation of replication stress signaling and apoptotic pathway activation at the protein level.

2.2.6. Molecular validation of cellular responses by western blot analysis

To corroborate the cytometric and functional findings at the molecular level, the expression of proteins associated with DNA damage response, cell-cycle regulation, and apoptosis was analyzed by Western

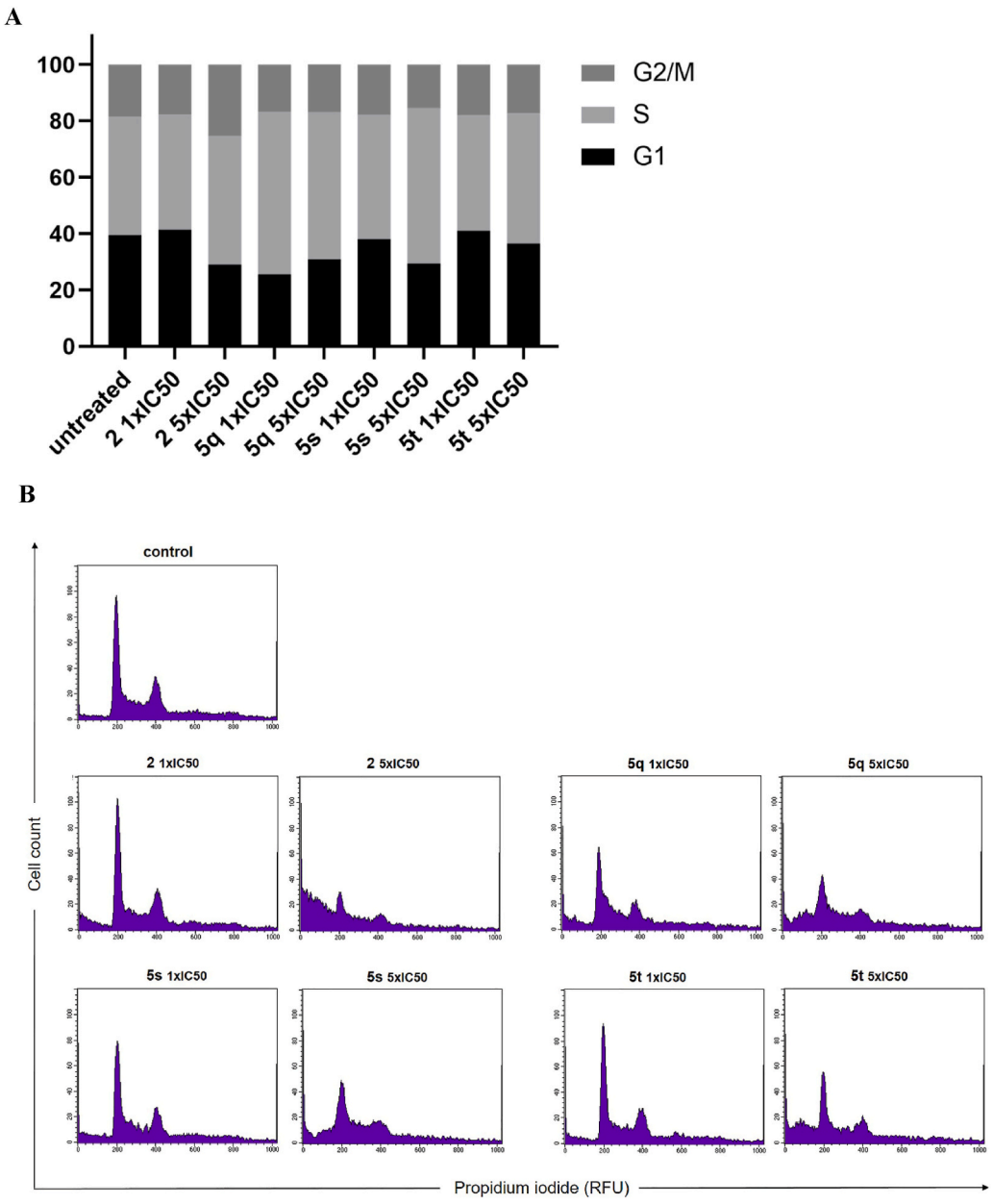

(caption on next page)

Fig. 3. Effects of selected compounds on cell-cycle distribution and mitotic activity in CCRF-CEM cells. (A) Quantitative analysis of cell cycle distribution in CCRF-CEM cells treated with compounds **2**, **5q**, **5s**, and **5t** at concentrations corresponding to 1× and 5 × IC_{50} for 24 h. DNA content was assessed by propidium iodide (PI) staining followed by flow-cytometric analysis. Bar graphs represent the relative proportions of cells in G1, S, and G2/M phases expressed as percentages of the total gated cell population. Untreated cells served as control. (B) Representative DNA content histograms corresponding to the conditions shown in panel (C) Analysis of mitotic cells by flow-cytometric detection of histone H3 phosphorylation at serine 10 (pH3Ser10) in CCRF-CEM cells treated with compounds **2**, **5q**, **5s**, and **5t** at 1× and 5 × IC_{50} for 24 h. Data are presented as the percentage of pH3Ser10-positive cells relative to the total gated population. Untreated cells were used as control.

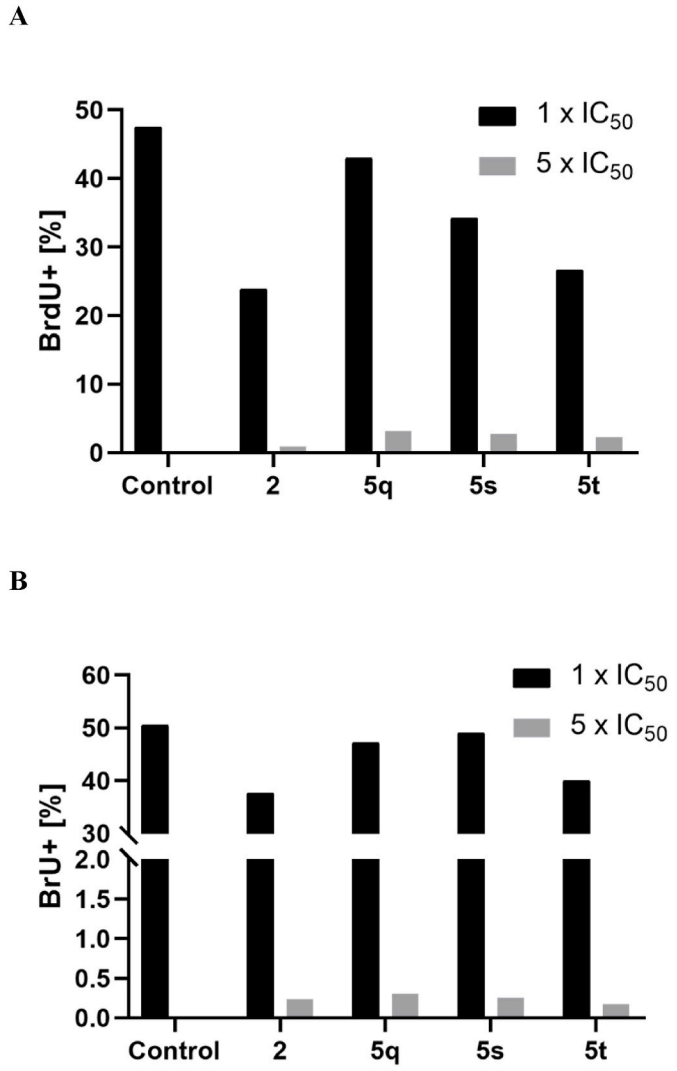

Fig. 4. Effects of selected compounds on DNA and RNA synthesis in CCRF-CEM cells. (A) Analysis of DNA synthesis in CCRF-CEM cells treated with compounds **2**, **5q**, **5s**, and **5t** at concentrations corresponding to 1 × and 5 × IC_{50} for 24 h. DNA replication activity was assessed by BrdU incorporation followed by flow-cytometric detection. Data are expressed as the percentage of BrdU-positive cells relative to the total gated population. Untreated cells served as control. (B) Analysis of RNA synthesis under the same experimental conditions. RNA synthesis was quantified by BrU incorporation followed by flow-cytometric analysis. Values represent the percentage of BrU-positive cells within the gated population. Untreated CCRF-CEM cells were used as control. Both DNA and RNA synthesis analyses were performed on intact cells selected by FSC/SSC gating to exclude debris and fragmented events.

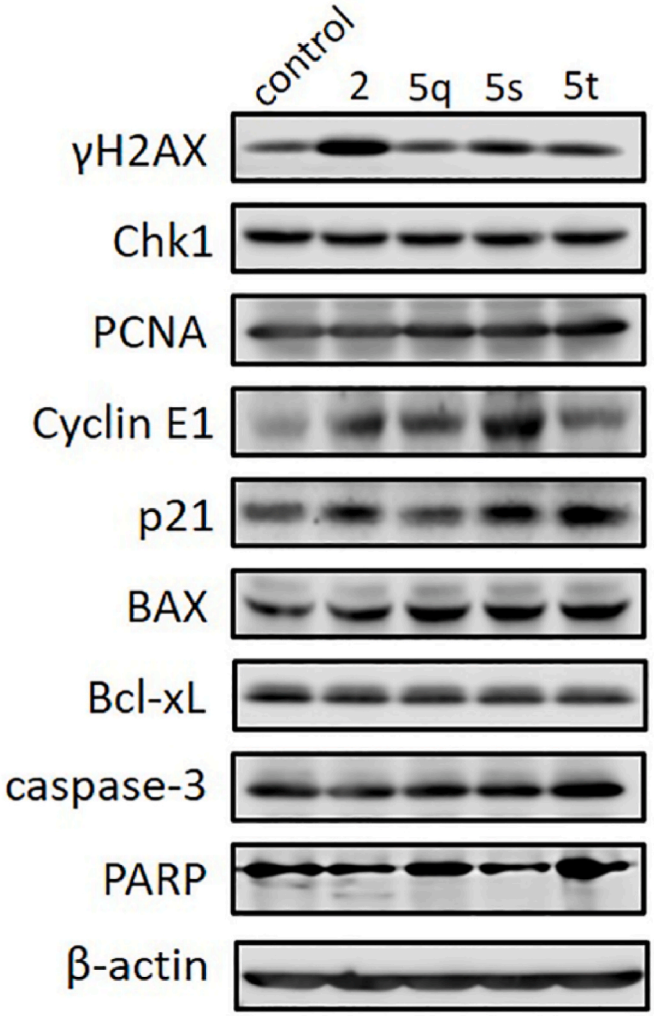

Fig. 5. Molecular characterization of cellular responses induced by selected compounds in CCRF-CEM cells. Expression of proteins associated with DNA damage response, cell-cycle regulation, and apoptosis was analyzed by Western blot in CCRF-CEM cells treated with compounds **2**, **5q**, **5s**, and **5t** at concentrations corresponding to 1× IC_{50} for 24 h. Representative immunoblots are shown for γH2AX (Ser139), Chk1, PCNA, Cyclin E1, p21, BAX, Bcl-xL, caspase-3, and PARP. β-actin was used as a loading control.

blot following 24 h treatment of CCRF-CEM cells with compounds **2**, **5q**, **5s**, and **5t** at concentrations corresponding to 1 × IC_{50} (Fig. 5). This treatment regimen was selected to capture early and intermediate stages of the cellular response while avoiding extensive cell loss and protein degradation observed at higher compound concentrations (5 × IC_{50}). Consistent with the strong suppression of DNA synthesis and pronounced S-phase accumulation described above (Sections 2.2.4 and 2.2.5), all tested compounds induced a clear increase in γH2AX (Ser139), indicating activation of the DNA damage response. The observed elevation of γH2AX strongly supports the presence of replication-associated DNA lesions, such as stalled or collapsed replication forks, and is in line with the functional evidence of impaired DNA synthesis. In contrast, the total expression of Chk1 remained largely unchanged across all treatments, suggesting that checkpoint activation may occur primarily at the post-translational level rather than via increased protein abundance, which is consistent with canonical ATR-Chk1 signaling during replication stress. Further support for

disruption of S-phase progression is provided by the marked upregulation of Cyclin E1 and p21. Increased Cyclin E1 expression reflects perturbation of S-phase dynamics and possible accumulation of cells at the G1/S transition or within early S phase, while the robust induction of p21 indicates activation of a stress-responsive checkpoint mechanism that restrains cell-cycle progression. Together, these changes provide a molecular basis for the S-phase enrichment observed in flow-cytometric analyses and further substantiate replication stress as a primary initiating event. In contrast, expression levels of PCNA remained largely stable, with only minor variability between individual treatments. This observation suggests that the replication machinery is not uniformly degraded or depleted but may instead be functionally impaired or stalled, consistent with the accumulation of cells in S phase rather than their exit from the cell cycle. Similarly, the absence of a consistent change in Chk1 protein levels further emphasizes that the observed cell-cycle perturbations are driven by functional modulation of existing signaling networks rather than gross changes in protein abundance. The transition from replication stress to apoptotic signaling is reflected by changes in mitochondrial pathway regulators. Notably, treatment with the tested compounds resulted in increased expression of the pro-apoptotic protein BAX, while levels of the anti-apoptotic protein Bcl-xL remained largely unchanged or only marginally reduced. This shift toward a pro-apoptotic balance is consistent with the mitochondrial depolarization observed in JC-1 assays (Section 2.2.3) and supports the engagement of the intrinsic apoptotic pathway at the level of mitochondrial outer membrane permeabilization. In contrast, markers of downstream apoptotic execution remained only weakly affected under the applied conditions. No substantial cleavage of caspase-3 was detected, and both pro-caspase-3 levels and the absence of its active fragments indicate that caspase-dependent execution of apoptosis is not yet fully established at 1× IC_{50} after 24 h. Similarly, full-length PARP showed only moderate reduction with minimal evidence of cleavage, limited primarily to compound **2**. These findings are fully consistent with the Annexin V/PI data, which demonstrated only a modest increase in apoptotic cell populations at this concentration, and suggest that cells are primarily in an early or pre-execution phase of apoptosis rather than undergoing widespread caspase-mediated cell death. Taken together, the Western blot data provide molecular validation of the mechanism inferred from cytometric analyses. The combined increase in γH2AX, Cyclin E1, p21, and BAX, alongside the absence of pronounced caspase activation, supports a model in which the tested compounds induce replication stress that leads to S-phase arrest and initiates mitochondrial apoptotic signaling without immediate execution of apoptosis. This temporal separation between upstream stress responses and downstream cell death is consistent with a stepwise mechanism in which prolonged replication stress ultimately culminates in caspase activation and irreversible apoptosis at later stages or higher compound concentrations.

2.2.7. *Pharmacological parameters*

To further evaluate the potential of the most active compounds **2**, **5q**, **5s**, **5t** for drug development, pharmacological parameters were measured. The rationale for the selection and detailed description of the measurement of these parameters has been reported earlier in Refs. [63, 64]. Compounds **2**, **5q**, **5s**, **5t** were selected for the measurement of *in vitro* pharmacological parameters (Table 2). These four candidates were selected to evaluate fundamental pharmacokinetic parameters such as absorption, distribution, metabolism, and excretion (ADME). Understanding the ADME properties of a new chemical entity is critical during its evaluation to become a leading candidate in a drug discovery program. The compounds were incubated with human plasma *in vitro* to quickly determine their susceptibility to plasma degradation and to what extent. All compounds demonstrated high stability in human plasma after 2 h incubation (86 to 100% of the original quantity of the substance remaining). Plasma protein binding was measured using Equilibrium Dialysis, studied compounds **2**, **5q**, **5s**, and **5t** were bound by 89%, 91%, 89%, and 87%, respectively. For the microsomal stability assay, human liver microsomes and NADPH cofactor were used to assess phase I oxidation by cytochrome P450 and flavin monooxygenases. The intrinsic clearance calculated from the microsomal stability assay indicated medium category. This means that studied compounds were not rapidly metabolized by liver microsome enzymes. The derivatives exhibited low ability (- log Papp >6 cm/s) to diffuse passively through an artificial cellular membrane in the Parallel Artificial Membrane Permeability Assay (PAMPA), suggesting an alternative intracellular transport mechanism might be involved. The Caco-2 and MDCK-MDR1 permeability assays are established models of intestinal [67] and blood-brain barriers, respectively [68]. It can be concluded that the

Table 2
Pharmacological parameters of compounds **2**, **5q**, **5s**, **5t**.

Compound	Plasma stability				Plasma protein binding	PAMPA	
	% Compound remaining					log Pe	Category[a]
	15 min	30	60	120	% Fraction bound		
2	100	97	95	86	89.25	−7.16	Low
5q	99	97	95	91	91.31	−7.32	Low
5s	100	98	98	97	88.64	−6.52	Low
5t	97	97	96	96	87.21	−6.96	Low

Compound	Microsomal stability			Microsomal stability
	% Compound remaining			Category of Intrinsic clearance[b]
	15 min	30	60	
2	80	70	67	Medium
5q	94	77	75	Medium
5s	83	78	76	Medium
5t	86	65	53	Medium

Compound	MDCK-MDR1 Permeability Assay					Caco-2 Permeability Assay				
	Papp (x10e-6)	Category	Efflux ratio	active efflux	% recovery	Papp (x10e-6)	Category	Efflux ratio	active efflux	% recovery
2	2.07	negative	2.7	Yes	92.37	1.34	Low	1.3	No	91.25
5q	1.21	negative	0.9	No	85.49	0.30	Low	0.8	No	88.96
5s	0.60	negative	0.8	No	93.21	0.65	Low	0.9	No	92.72
5t	1.21	negative	1.1	No	87.39	0.66	Low	1.4	No	91.08

[a,b]References [65,66], error deviations are within a range of values less than 10% (all experiments were done in triplicates, except for cell-based permeability assays, which were performed in duplicates).

studied molecules exhibited low (PappAB <5×10-6 cm/s) probability of intestinal absorption and crossing the blood-brain barrier (PappAB <10×10-6 cm/s).

We assessed rates of transport across Caco-2 and MDCK-MDR1 monolayers in both directions (apical to basolateral (A-B) and basolateral to apical (B-A)) across the cell monolayer, which enabled us to determine the efflux ratio and assess whether the compound undergoes active efflux. The derivatives studied were not actively exported from the cells in both barrier models, as indicated by efflux ratios ER < 2, the only exception was a limited active transport of compound **2** with ER 2.7. Results from all *in vitro* pharmacology testing are summarized in Table 2.

3. Conclusions

The primary objective of this study was to explore the synthetic pathways for the preparation of amino derivatives of betulin diacetate (**1**), aimed at the improvement of its polarity while retaining or increasing its selective cytotoxicity in cancer cells. To date, literature precedents regarding the introduction of an amine moiety at the C-30 position of betulin diacetate (**1**) remain scarce, almost exclusively relying on an allylic bromination–substitution sequence. This approach is inefficient, since the radical bromination using NBS in CCl_4 gives only modest yields [46,61] and utilizes toxic and environmentally hazardous solvent. Consequently, a key specific aim of this project was to substitute this procedure by Tsuji-Trost amination protocol to circumvent these limitations. As a result, three sets of new amino derivatives were obtained (**5a** – **5x**, **6a**, **6b**, **7a** – **7e**) in moderate to high yield. The wide scope of the procedure was shown by numerous substituents used and by the fact that secondary, tertiary, and cyclic amines were prepared.

All synthesized compounds were screened for their *in vitro* cytotoxic activity against six cancer and two non-cancerous cell lines. Among these, compounds **2**, **5q**, **5s**, and **5t**, were selected for subsequent detailed biological evaluation. All four had IC_{50} values within the low-micromolar or even submicromolar range in CCRF-CEM cell line, as well as a strong effects in K562, and moderate activity across selected solid tumor lines. Their IC_{50} values in non-cancer fibroblasts (BJ, MRC-5) remained slightly higher, yielding a therapeutically remained slightly higher, yielding a therapeutically narrower selectivity window. Beyond the primary hits, a small subset of derivatives, including **5d**, **5g**, **5i**, and **5p**, were selectively cytotoxic to hematological cancer models, while remaining largely inactive toward fibroblasts and most solid tumor lines.

Mechanistic characterization of the lead compounds revealed that their antiproliferative activity is driven by a well-defined and highly coordinated cellular response. Flow-cytometric analyses demonstrated pronounced S-phase accumulation accompanied by strong inhibition of DNA synthesis, identifying replication stress as the primary cellular insult. This was further supported by induction of γH2AX and upregulation of Cyclin E1 and p21, consistent with activation of DNA damage-associated checkpoint signaling. Apoptotic assays indicated that cell death is initiated through the mitochondrial pathway, as evidenced by loss of membrane potential and increased BAX expression, while minimal caspase activation and limited PARP cleavage suggest that cells predominantly undergo early apoptotic commitment rather than full execution under the applied conditions. Collectively, the data support a mechanism in which replication stress leads to S-phase arrest and subsequently triggers mitochondria-dependent apoptosis.

From a therapeutic perspective, the preferential activity of these compounds toward hematological malignancies highlights replication-associated vulnerabilities as a promising target space. Future studies will focus on identifying the direct molecular targets responsible for replication stress induction, as well as on validation in more complex biological systems and exploration of combination strategies with DNA damage response modulators.

4. Experimental procedures

4.1. Chemistry

All reagents were of reagent grade and were used without further purification. Starting betulin diacetate in purity 98% was purchased from the company Betulinines (www.betulinines.com). All other chemicals and solvents including dry ones were purchased from Merck (Germany). The course of the reactions was monitored by TLC on Kieselgel 60 F_{254} plates (Merck, Germany) and detected by UV light (254 nm) followed by visualization using 10% aqueous H_2SO_4 and heating process to 150–200 °C. Purification was performed using column chromatography on Silica gel 60 Merck 7734 (Merck, Germany). All ^1H and ^{13}C NMR experiments were recorded at 500 MHz (Jeol JNM-ECX-500) or 400 MHz (Jeol JNM-ECA400II) for ^1H NMR, and 126 MHz or 100 MHz for ^{13}C NMR, respectively, at 25 °C in CDCl3. Chemical shifts δ are reported relative to the residual solvent peak (for CDCl3 $\delta_H = 7.26$ ppm, $\delta_C = 77.16$ ppm). Chemical shifts δ are reported in parts per million (ppm) and coupling constants J are reported in Hertz (Hz). HRMS analyses were performed on a SELECT SERIES Cyclic IMS QTOF (Waters Corp., Wilmslow, U.K.) equipped with an Atmospheric Solid Analysis Probe (ASAP) source operated in positive mode. Sodium iodide 2 μg/μL in propan-2-ol/water (1:1, v/v) was used for the mass calibration (m/z 50−2000). Instrumental parameters were set as follows: corona current 2 μA and desolvation temperature of 400 °C under standard condition and 500 °C for less efficiently ionizing analytes, respectively. Data were acquired with a lockmass correction using leucine enkephalin at a concentration of 50 pg/μL in water/acetonitrile (1:1, v/v) containing 0.1% formic acid, monitoring the $[M + H]^+$ ion at m/z 556.2771. Samples were dissolved in acetone and analyzed at a concentration of 10 μg/mL, with an increased concentration of 50 μg/mL applied for compounds exhibiting poorer ionization efficiency. For ASAP introduction, a quartz capillary was immersed directly into the sample solution and subsequently positioned in the ASAP source for direct analysis. IR samples were analyzed by Fourier transform infrared spectroscopy in attenuated total reflectance (ATR) mode using a Nicolet iS50 FTIR spectrometer (Thermo Fisher Scientific). Optical rotations were measured on an ATAGO Automatic Compact Polarimeter POL-1/2 at 589 nm using a 10 mm cell; concentrations are given in g/100 mL.

4.1.1. Synthesis of 3β,28-diacetoxylup-20(29)-en-30-al (2)

Prepared following a previously published procedure [57]. Betulin diacetate (10.2 g; 98%; 0.019 mol) was dissolved in mixture of DCM (132 mL) and AcOH (78 mL). Both 70% aqueous solution of *tert*-Butyl hydroperoxide (7.8 mL; 0.057 mol) and Selenium dioxide (632 mg; 0.0057 mol) were then added into the reaction mixture. The reaction mixture was stirred at room temperature for 48 h. The reaction was determined to be complete by TLC analysis using mobile phase hexane/EtOAc (4:1). The reaction mixture was diluted with DCM (200 mL). Organic phase was washed three times with 1M solution of $FeSO_4 \cdot 7H_2O$ (250 mL), two times with saturated solution of $NaHCO_3$ (250 mL) and once with brine (200 mL). The organic phase was dried over anhydrous $MgSO_4$, and the organic solvent was subsequently removed under reduced pressure using a rotary evaporator, followed by column chromatography purification on SiO_2 eluting with a gradient mobile phase of hexane/EtOAc (7:1 to 4:1). After the purification process aldehyde was obtained in 84% yield as a white solid. $R_f = 0.54$ (hexane/EtOAc 4:1). $[\alpha]_D^{25} = +7.7$ (c = 1.0, THF). ^1H NMR (500 MHz, $CDCl_3$): δ 9.50 (s, 1H, CHO), 6.27 (s, 1H, H-29), 5.92 (s, 1H, H-29), 4.47 – 4.42 (m, 1H, H-3), 4.27 (d, $J = 11.2$ Hz, 1H, H-28), 3.86 (d, $J = 11.1$ Hz, 1H, H-28), 2.89 – 2.69 (m, 1H, H-19), 2.06 (s, 3H, $CH_3C{=}O$), 2.03 (s, 3H, $CH_3C{=}O$), 1.01 (s, 3H, CH_3), 0.93 (s, 3H, CH_3), 0.84 – 0.81 (m, 9H, 3 × CH_3). ^{13}C NMR (126 MHz, $CDCl_3$): δ 194.8 (-**C**H=O), 171.6 (-C=O, ester), 171.1 (-C=O, ester), 156.7 (C-20), 133.4 (C-29), 81.0 (C-3), 62.6 (-CH_2-OAc), 55.5, 50.2, 46.7, 42.7, 41.0, 38.5, 37.9, 37.4, 37.3, 37.2, 34.6, 34.2, 32.2,

29.9, 28.1, 27.6, 27.1, 23.8, 21.4, 21.2, 20.9, 18.3, 16.6, 16.2, 16.1, 14.7, 14.3. IR (DRIFT): 2938.56, 2868.40, 1736.71, 1722.09, 1687.35, 1460.32, 1389.86, 1365.05, 1235.03, 1028.61, 1014.09. HRMS (ASAP, TOF ES$^+$): calcd. for $C_{34}H_{53}O_5^+$ [M + H]$^+$ 541.3888, found 541.3896. The analytical data also compared with those reported in previously published research [69].

4.1.2. Synthesis of 3β,28-diacetoxy-30-hydroxylup-20(29)-ene (3)

Prepared following a previously published procedure [57]. Aldehyde (6.44 g; 0.012 mol) and $CeCl_3{\cdot}7H_2O$ (8 g; 0.0216 mol) were dissolved in mixture of THF (120 mL) and MeOH (40 mL). Sodium borohydride (817 mg, 0.0216 mol) was then added into the reaction mixture in small doses. The reaction mixture was stirred at room temperature for 15 min, after the complete addition of the sodium borohydride. The reaction was determined to be complete by TLC analysis using mobile phase hexane/EtOAc (3:1). The reaction mixture was diluted EtOAc (180 mL) and 1M solution of HCl (90 mL) was added. After phase separation, the aqueous layer was re-extracted with an additional portion of EtOAc (60 mL). The combined organic extracts were then washed once with H_2O (90 mL) and after that once with brine (90 mL). The organic phase was dried over anhydrous $MgSO_4$, and the organic solvent was subsequently removed under reduced pressure using a rotary evaporator, followed by column chromatography purification on SiO_2 eluting with a gradient mobile phase of hexane/EtOAc (4:1 to 2:1). After the purification process hydroxy derivative **2** was obtained in 78% yield as a white solid. $R_f = 0.31$ (hexane/EtOAc 3:1). $[\alpha]_D^{25} = -3.2$ (c = 1.0, THF). ^{1}H NMR (500 MHz, $CDCl_3$): δ 4.96 (d, J = 1.1 Hz, 1H, H-29), 4.90 (s, 1H, H-29), 4.48 – 4.44 (m, 1H, H-3), 4.23 (dd, J = 11.2, 1.4 Hz, 1H, H-28), 4.15 – 4.07 (m, 2H, H-30), 3.84 (d, J = 11.0 Hz, 1H, H-28), 2.34 (td, J = 11.0, 5.5 Hz, 1H, H-19), 2.06 (s, 3H, $CH_3C{=}O$), 2.03 (s, 3H, $CH_3C{=}O$), 1.03 (s, 3H, CH_3), 0.97 (s, 3H, CH_3), 0.85 – 0.83 (m, 6H, 2 × CH_3), 0.83 (s, 3H). ^{13}C NMR (126 MHz, $CDCl_3$): δ 171.7 (-C=O, ester), 171.1 (-C=O, ester), 154.4 (C-20), 107.4 (C-29), 81.0 (C-3), 65.1 (C-30), 62.6 (-**C**H$_2$-OAc), 55.5, 50.4, 49.6, 46.5, 43.6, 42.8, 41.1, 38.5, 37.9, 37.6, 37.2, 34.5, 34.3, 31.7, 29.9, 28.1, 27.2, 26.8, 23.8, 21.4, 21.2, 21.0, 18.3, 16.6, 16.3, 16.2, 14.9. IR (DRIFT): 3552.05, 2939.03, 2870.45, 1731.97, 1712.75, 1456.62, 1363.27, 1242.00, 1030.27, 1013.20. HRMS (ASAP, TOF ES$^+$): calcd. for $C_{34}H_{55}O_5^+$ [M + H]$^+$ 543.4044, found 543.4021. The analytical data also compared with those reported in previously published research [53].

4.1.3. Synthesis of 3β,28,30-triacetoxylup-20(29)-ene (4)

The Acetylation reaction was performed under inert conditions. Compound **2** (6.0 g; 0.011 mol) was dissolved in mixture of Ac_2O (20 mL) and Py (anhydrous; 25 mL). The reaction mixture was stirred at room temperature for 24 h. The reaction was determined to be complete by TLC analysis using mobile phase hexane/EtOAc (2:1). The reaction mixture was diluted EtOAc (245 mL) and was washed 6 times with 1M HCl (60 mL) and 2 times brine (60 mL). After phase separation, the organic phase was dried over anhydrous $MgSO_4$, and the organic solvent was subsequently removed under reduced pressure using a rotary evaporator, followed by column chromatography purification on SiO_2 eluting with a mobile phase of hexane/EtOAc (2:1). After the purification process ester derivative **3** was obtained in 95% yield as a white solid. $R_f = 0.33$ (hexane/EtOAc 6:1). $[\alpha]_D^{25} = -5.6$ (c = 1.0, THF). ^{1}H NMR (500 MHz, $CDCl_3$): δ 4.95 (s, 1H, H-29), 4.94 (d, J = 1.3 Hz, 1H, H-29), 4.56 (d, J = 13.6 Hz, 1H, H-30), 4.52 (d, J = 13.4 Hz, 1H, H-30), 4.49 – 4.43 (m, 1H, H-3), 4.24 (dd, J = 11.1, 1.2 Hz, 1H, H-28), 3.82 (d, J = 11.1 Hz, 1H, H-28), 2.36 (dt, J = 11.2, 5.6 Hz, 1H, H-19), 2.09 (s, 3H, $CH_3C{=}O$), 2.06 (s, 3H, $CH_3C{=}O$), 2.03 (s, 3H, $CH_3C{=}O$), 1.03 (s, 3H, CH_3), 0.97 (s, 3H, CH_3), 0.86 – 0.83 (m, 6H, 2 × CH_3), 0.83 (s, 3H, CH_3). ^{13}C NMR (126 MHz, $CDCl_3$): δ 171.7 (-C=O, ester), 171.1 (-C=O, ester), 170.8 (-C=O, ester), 148.9 (C-20), 110.8 (C-29), 81.0 (C-3), 66.1 (-**C**H$_2$-OAc), 62.6 (-**C**H$_2$-OAc), 55.5, 50.4, 49.6, 46.5, 44.0, 42.8, 41.1, 38.5, 37.9, 37.6, 37.2, 34.5, 34.3, 31.2, 29.9, 28.1, 27.2, 26.7, 23.8, 21.5, 21.2, 21.0, 18.3, 16.6, 16.3, 16.2, 14.9. IR (DRIFT): 2932.31, 2872.49, 1732.27, 1458.27, 1364.44, 1226.72, 1027.83. HRMS (ASAP, TOF ES$^+$): calcd. for $C_{36}H_{57}O_6^+$ [M + H]$^+$ 585.4150, found 585.4149. The analytical data obtained in this study were compared with those reported in previously published research [53].

4.1.4. General procedure for Tsuji-Trost reaction

The Tsuji-Trost reaction was performed under inert conditions and using degassed solvents. Ester **3** (250 mg; 0.427 mmol); appropriate amine (1.708 mmol) and K_2CO_3 (118 mg; 0.854 mmol) were dissolved in degassed mixture of THF (2.5 mL) and H_2O (2.5 mL). After that Pd(OAc)$_2$ (4.8 mg; 0.02135 mmol) and TPPTS (61 mg; 0.10675 mmol) were added into the reaction mixture. The reaction mixture was stirred at 60 °C. The exact reaction time depended on used amine and is specified for each derivative. The completion of reaction was determined by TLC analysis using mobile phase hexane/EtOAc (6:1). The reaction mixture was diluted with EtOAc (40 mL). Organic phase was washed twice with H_2O (10 mL) and once with brine (20 mL). The organic phase was dried over anhydrous $MgSO_4$, and the organic solvent was subsequently removed under reduced pressure using a rotary evaporator, followed by column chromatography purification on SiO_2 eluting with organic solvents (details will be specified for each derivative).

4.1.5. Synthesis of secondary amines 5a-5x

4.1.5.1. 3β,28-diacetoxy-30-(butylamino)lup-20(29)-ene (5a). Compound (**5a**) was prepared according to the general procedure for Tsuji-Trost reaction. The reaction time was 24 h. After the column chromatography purification using EtOAc derivative **5a** was obtained in 81% yield as a white solid. $R_f = 0.26$ (EtOAc). $[\alpha]_D^{25} = -3.0$ (c = 1.0, THF). ^{1}H NMR (500 MHz, $CDCl_3$): δ 4.86 – 4.82 (m, 2H, 2 × H-29), 4.49 – 4.43 (m, 1H, H-3), 4.24 (dd, J = 11.1, 1.0 Hz, 1H, H-28a), 3.84 (d, J = 11.0 Hz, 1H, H-28b), 3.21 (d, J = 15.2 Hz, 1H, H-30a), 3.14 (d, J = 15.2 Hz, 1H, H-30b), 2.66 – 2.56 (m, 2H, CH_2), 2.33 (td, J = 10.4, 5.3 Hz, 1H, H-19), 2.06 (s, 3H, $CH_3C{=}O$), 2.03 (s, 3H, $CH_3C{=}O$), 1.02 (s, 3H, CH_3), 0.96 (s, 3H, CH_3), 0.92 (t, J = 7.3 Hz, 3H, CH_3), 0.84 (s, 6H, 2 × CH_3), 0.83 (s, 3H, CH_3). ^{13}C NMR (126 MHz, $CDCl_3$): δ 171.7 (-C=O, ester), 171.1 (-C=O, ester), 153.0 (C-20), 107.4 (C-29), 81.0 (C-3), 62.8 (-**C**H$_2$-OAc), 55.5, 53.5, 50.4, 49.7, 49.5, 46.4, 45.2, 42.8, 41.1, 38.5, 37.9, 37.6, 37.2, 34.6, 34.3, 32.5, 31.5, 29.9, 28.1, 27.2, 26.6, 23.8, 21.5, 21.2, 21.0, 20.7, 18.3, 16.6, 16.3, 16.2, 14.9, 14.2. IR (DRIFT): 2941.04, 2874.54, 1732.25, 1456.58, 1364.08; 1237.14, 1028.44. HRMS (ASAP, TOF ES$^+$): calcd. for $C_{38}H_{64}NO_4^+$ [M + H]$^+$ 598.4830, found 598.4847.

4.1.5.2. 3β,28-diacetoxy-30-[(3-tert-butoxy-3-oxopropyl)amino]lup-20(29)-ene (5b). Compound (**5b**) was prepared according to the general procedure for Tsuji-Trost reaction. The reaction time was 24 h. After the column chromatography purification using EtOAc derivative **5b** was obtained in 71% yield as a white solid. $R_f = 0.67$ (EtOAc). $[\alpha]_D^{25} = +2.2$ (c = 1.0, THF). ^{1}H NMR (500 MHz, $CDCl_3$): δ 4.88 – 4.82 (m, 2H, H-29), 4.48 – 4.43 (m, 1H, H-3), 4.24 (dd, J = 11.1, 1.0 Hz, 1H, H-28a), 3.83 (d, J = 11.1 Hz, 1H, H-28b), 3.21 (d, J = 15.2 Hz, 1H, H-30a), 3.14 (d, J = 15.1 Hz, 1H, H-30b), 2.84 (h, J = 5.5 Hz, 2H, CH_2), 2.44 (t, J = 6.5 Hz, 2H, CH_2), 2.34 (td, J = 10.1, 4.7 Hz, 1H, H-19), 2.06 (s, 3H, $CH_3C{=}O$), 2.03 (s, 3H, $CH_3C{=}O$), 1.45 (s, 9H, 3 × CH_3), 1.02 (s, 3H, CH_3), 0.96 (s, 3H, CH_3), 0.84 (s, 6H, 2 × CH_3), 0.83 (s, 3H, CH_3). ^{13}C NMR (126 MHz, $CDCl_3$): δ 172.4 (-C=O, ester), 171.7 (-C=O, ester), 171.1 (-C=O, ester), 152.8 (C-20), 107.6 (C-29), 81.1 (C-3), 80.6 (-O-**C**(CH$_3$)$_3$), 62.8 (-**C**H$_2$-OAc), 55.5, 53.3, 50.4, 49.5, 46.4, 45.2, 42.8, 41.1, 38.5, 37.9, 37.6, 37.2, 36.1, 34.6, 34.3, 31.5, 29.9, 29.8, 28.3, 28.1, 27.2, 26.6, 23.8, 21.5, 21.2, 21.0, 18.3, 16.6, 16.3, 16.2, 14.9. IR (DRIFT): 2941.46, 2868.40, 1728.46, 1456.75, 1389.93, 1364.80, 1239.31, 1152.84, 1028.68. HRMS (ASAP, TOF ES$^+$): calcd. for $C_{41}H_{68}NO_6^+$ [M + H]$^+$ 670.5041, found 670.5059.

*4.1.5.3. 3β,28-diacetoxy-30-[(2-tert-butoxy-2-oxoethyl)amino]lup-20 (29)-ene (**5c**).* Compound (**5c**) was prepared according to the general procedure for Tsuji-Trost reaction. The reaction time was 48 h. After the column chromatography purification using hexane/EtOAc (3:2) derivative **5c** was obtained in 13% yield as a white solid. $R_f = 0.57$ (hexane/EtOAc 3:2). ^{1}H NMR (500 MHz, $CDCl_3$): δ 4.91 – 4.82 (m, 2H, H-29), 4.49 – 4.43 (m, 1H, H-3), 4.24 (dd, $J = 11.2$, 1.0 Hz, 1H, H-28a), 3.83 (d, $J = 11.1$ Hz, 1H, H-28b), 3.35 – 3.25 (m, 2H, CH_2), 3.20 (d, $J = 14.8$ Hz, 1H, H-30a), 3.13 (d, $J = 14.9$ Hz, 1H, H-30b), 2.41 – 2.29 (m, 1H, H-19), 2.06 (s, 3H, CH_3C=O), 2.03 (s, 3H, CH_3C=O), 1.47 (s, 9H, 3 × CH_3), 1.02 (s, 3H, CH_3), 0.96 (s, 3H, CH_3), 0.84 (s, 6H, 2 × CH_3), 0.83 (s, 3H, CH_3). ^{13}C NMR (126 MHz, $CDCl_3$): δ 171.9 (-C=O, ester), 171.7 (-C=O, ester), 171.1 (-C=O, ester), 152.3 (C-20), 108.1 (C-29), 81.3 (-O-**C**$(CH_3)_3$), 81.1 (C-3), 62.7 (-**C**H_2-OAc), 55.5, 51.3, 50.4, 49.5, 46.5, 45.1, 42.8, 41.1, 38.5, 37.9, 37.6, 37.2, 34.6, 34.3, 31.5, 29.9, 29.8, 28.3, 28.1, 27.2, 26.6, 23.8, 21.5, 21.2, 21.0, 18.3, 16.6, 16.3, 16.2, 14.9. IR (DRIFT): 2942.55, 2866.35, 1731.25, 1458.27, 1390.52, 1365.39, 1236.59, 1154.75, 1028.86. HRMS (ASAP, TOF ES$^+$): calcd. for $C_{40}H_{66}NO_6^+$ $[M + H]^+$ 656.4885, found 656.4883.

*4.1.5.4. 3β,28-diacetoxy-30-[(6-deoxy-1,2:3,4-di-O-isopropylidene-α-D-galactopyranos-6-yl)amino]lup-20(29)-ene (**5d**).* Amine precursor was synthetized according to the previously reported two-step process via azide [70] and its reduction [71]. Compound (**5d**) was prepared according to the general procedure for Tsuji-Trost reaction. The reaction time was 24 h. After the column chromatography purification using hexane/EtOAc (1:1) derivative **5d** was obtained in 80% yield as a white solid. $R_f = 0.28$ (hexane/EtOAc 1:1). ^{1}H NMR (500 MHz, $CDCl_3$): δ 5.53 (d, $J = 5.0$ Hz, 1H), 4.88 (d, $J = 0.8$ Hz, 1H, H-29), 4.84 (s, 1H, H-29), 4.59 (dd, $J = 7.9$, 2.3 Hz, 1H), 4.49 – 4.44 (m, 1H, H-3), 4.31 (dd, $J = 5.1$, 2.3 Hz, 1H), 4.24 (d, $J = 11.2$ Hz, 1H, H-28a), 4.20 (dd, $J = 7.9$, 1.9 Hz, 1H), 3.94 (ddd, $J = 8.5$, 4.0, 1.9 Hz, 1H), 3.82 (d, $J = 10.8$ Hz, 1H, H-28b), 3.24 (d, $J = 15.2$ Hz, 1H, H-30a), 3.14 (d, $J = 15.2$ Hz, 1H, H-30b), 2.91 (dd, $J = 12.5$, 8.6 Hz, 1H), 2.77 (dd, $J = 12.5$, 4.0 Hz, 1H), 2.41 – 2.24 (m, 1H, H-19), 2.06 (s, 3H, CH_3C=O), 2.03 (s, 3H, CH_3C=O), 1.54 (s, 3H, CH_3), 1.45 (s, 3H, CH_3), 1.34 (s, 3H, CH_3), 1.33 (s, 3H, CH_3), 1.02 (s, 3H, CH_3), 0.95 (s, 3H, CH_3), 0.84 (s, 6H, 2 × CH_3), 0.83 (s, 3H, CH_3). ^{13}C NMR (126 MHz, $CDCl_3$): δ 171.7 (-C=O, ester), 171.1 (-C=O, ester), 152.7 (C-20), 109.3 (-**C**$(CH_3)_2$, acetonide carbon), 108.6 (-**C**$(CH_3)_2$, acetonide carbon), 107.8 (C-29), 96.5 (anomeric **C**), 81.0 (C-3), 72.2 (pyranose **C**H), 71.0 (pyranose **C**H), 70.8 (pyranose **C**H), 67.2 (pyranose **C**H), 62.8 (-**C**H_2-OAc), 55.5, 50.4, 49.5, 46.4, 42.8, 41.1, 38.5, 37.9, 37.6, 37.2, 34.6, 34.3, 31.5, 29.9, 29.8, 28.1, 27.2, 26.6, 26.3, 26.2, 25.1, 24.5, 23.8, 22.8, 21.5, 21.2, 21.0, 18.3, 16.6, 16.3, 16.2, 14.9, 14.3. IR (DRIFT): 2941.30, 2868.40, 1732.29, 1636.14, 1596.02, 1471.31, 1371.23, 1329.41, 1242.41, 1155.72, 1076.61, 1029.67. HRMS (ASAP, TOF ES$^+$): calcd. for $C_{46}H_{74}NO_9^+$ $[M + H]^+$ 784.5358, found 784.5367.

*4.1.5.5. 3β,28-diacetoxy-30-[(5′-deoxy-2′,3′-O-isopropylideneadenosin-5′-yl)amino]lup-20(29)-ene (**5e**).* Amine precursor was synthetized according to the previously reported two-step process via azide [72] and its reduction [73]. Compound (**5e**) was prepared according to the general procedure for Tsuji-Trost reaction. The reaction time was 24 h. After the column chromatography purification using EtOAc derivative **5e** was obtained in 50% yield as a white solid. $R_f = 0.19$ (EtOAc). $[\alpha]_D^{25} = -15.2$ (c = 1.0, THF). ^{1}H NMR (500 MHz, $CDCl_3$): δ 8.32 (s, 1H, aryl), 7.90 (s, 1H, aryl), 5.99 (d, $J = 3.3$ Hz, 1H), 5.73 (s, 2H), 5.47 (dd, $J = 6.4$, 3.3 Hz, 1H), 5.08 (dd, $J = 6.5$, 3.3 Hz, 1H), 4.84 – 4.79 (m, 2H, H-29), 4.50 – 4.43 (m, 1H, H-3), 4.42 – 4.37 (m, 1H), 4.23 (d, $J = 11.0$ Hz, 1H, H-28a), 3.80 (d, $J = 11.1$ Hz, 1H, H-28b), 3.21 (d, $J = 15.0$ Hz, 1H, H-30a), 3.12 (d, $J = 15.0$ Hz, 1H, H-30b), 2.93 (dd, $J = 12.6$, 3.9 Hz, 1H), 2.86 (dd, $J = 12.5$, 5.9 Hz, 1H), 2.37 – 2.20 (m, 1H, H-19), 2.06 (s, 3H, CH_3C=O), 2.03 (s, 3H, CH_3C=O), 1.61 (s, 3H, CH_3), 1.38 (s, 3H, CH_3), 0.99 (s, 3H, CH_3), 0.93 (s, 3H, CH_3), 0.83 (s, 3H, CH_3), 0.83 – 0.80 (m, 6H, 2 × CH_3). ^{13}C NMR (126 MHz, $CDCl_3$): δ 171.8 (-C=O, ester), 171.2 (-C=O, ester), 155.7 (C-aryl), 153.3 (C-aryl), 152.4 (C-20), 149.6 (C-aryl), 140.1 (C-aryl), 120.6 (C-aryl), 114.7 (-**C**$(CH_3)_2$, acetonide carbon), 108.0 (C-29), 91.1 (anomeric **C**), 85.6 (ribose **C**H), 83.5 (ribose **C**H), 82.3 (ribose **C**H), 81.1 (C-3), 62.8 (-**C**H_2-OAc), 55.5, 53.6, 51.1, 50.4, 49.4, 46.4, 44.9, 42.8, 41.0, 38.5, 37.9, 37.6, 37.2, 34.5, 34.3, 31.5, 29.9, 28.1, 27.5, 27.2, 26.6, 25.6, 23.8, 21.5, 21.2, 21.0, 18.3, 16.6, 16.3, 16.1, 14.9. IR (DRIFT): 2942.55, 2866.35, 1731.25, 1458.27, 1390.52, 1365.39, 1236.59, 1154.75, 1028.86. HRMS (ASAP, TOF ES+): calcd. for $C_{47}H_{71}N_6O_7^+$ $[M + H]^+$ 831.5379, found 831.5392.

*4.1.5.6. 3β,28-diacetoxy-30-benzylaminolup-20(29)-ene (**5f**).* Compound (**5f**) was prepared according to the general procedure for Tsuji-Trost reaction. The reaction time was 24 h. After the column chromatography purification using hexane/EtOAc (3:2) derivative **5f** was obtained in 66% yield as a white solid. $R_f = 0.50$ (hexane/EtOAc 3:2). $[\alpha]_D^{25} = -3.0$ (c = 1.0, THF). ^{1}H NMR (500 MHz, $CDCl_3$): δ 7.35 – 7.31 (m, 4H, aryl), 7.27 – 7.23 (m, 1H, aryl), 4.91 (d, $J = 1.3$ Hz, 1H, H-29), 4.88 (s, 1H, H-29), 4.50 – 4.45 (m, 1H, H-3), 4.24 (dd, $J = 11.2$, 1.3 Hz, 1H, H-28a), 3.85 – 3.77 (m, 3H, H-28b, AB system of -CH_2-Ph), 3.24 (d, $J = 15.0$ Hz, 1H, H-30a), 3.18 (d, $J = 14.9$ Hz, 1H, H-30b), 2.37 (td, $J = 11.0$, 5.2 Hz, 1H, H-19), 2.06 (s, 3H, CH_3C=O), 2.04 (s, 3H, CH_3C=O), 1.02 (s, 3H, CH_3), 0.93 (s, 3H, CH_3), 0.85 (s, 6H, 2 × CH_3), 0.84 (s, 3H, CH_3). ^{13}C NMR (126 MHz, $CDCl_3$): δ 171.7 (-C=O, ester), 171.1 (-C=O, ester), 152.9 (C-20), 140.7 (C-aryl), 128.5 (C-aryl), 128.2 (C-aryl), 127.1 (C-aryl), 108.0 (C-29), 81.1 (C-3), 62.8 (-**C**H_2-OAc), 55.5, 53.7, 52.9, 50.4, 49.6, 46.5, 45.2, 42.8, 41.1, 38.6, 38.0, 37.7, 37.2, 34.6, 34.3, 31.6, 29.9, 28.1, 27.2, 26.6, 23.9, 21.5, 21.2, 21.1, 18.3, 16.6, 16.3, 16.2, 14.9. IR (DRIFT): 2940.92, 2866.35, 1731.49, 1454.18, 1363.81, 1239.57, 1027.88. HRMS (ASAP, TOF ES$^+$): calcd. for $C_{41}H_{62}NO_4^+$ $[M + H]^+$ 632.4673, found 632.4683. The analytical data obtained in this study were compared with those reported in previously published research [41].

*4.1.5.7. 3β,28-diacetoxy-30-(4-methylbenzylamino)lup-20(29)-ene (**5g**).* Compound (**5g**) was prepared according to the general procedure for Tsuji-Trost reaction. The reaction time was 24 h. After the column chromatography purification using hexane/EtOAc (3:2) derivative **5g** was obtained in 78% yield as a white solid. $R_f = 0.38$ (hexane/EtOAc 3:2). $[\alpha]_D^{25} = -5.2$ (c = 1.0, THF). ^{1}H NMR (500 MHz, $CDCl_3$): δ 7.23 – 7.21 (m, 2H, aryl), 7.15 – 7.12 (m, 2H, aryl), 4.90 (d, $J = 1.2$ Hz, 1H, H-29), 4.87 (s, 1H, H-29), 4.49 – 4.45 (m, 1H, H-3), 4.24 (dd, $J = 11.1$, 1.1 Hz, 1H, H-28a), 3.83 (d, $J = 11.0$ Hz, 1H, H-28b), 3.78 (d, $J = 13.1$ Hz, 1H, part of AB system -CH_2-Ar), 3.74 (d, $J = 13.1$ Hz, 1H, part of AB system -CH_2-Ar), 3.23 (d, $J = 14.9$ Hz, 1H, H-30a), 3.17 (d, $J = 14.9$ Hz, 1H, H-30b), 2.39 – 2.32 (m, 4H, H-19, Ar-CH_3), 2.06 (s, 3H, CH_3C=O), 2.04 (s, 3H, CH_3C=O), 1.02 (s, 3H, CH_3), 0.93 (s, 3H, CH_3), 0.85 (s, 6H, 2 × CH_3), 0.84 (s, 3H, CH_3). ^{13}C NMR (126 MHz, $CDCl_3$): δ 171.7 (-C=O, ester), 171.1 (-C=O, ester), 153.0 (C-20), 137.6 (C-aryl), 136.6 (C-aryl), 129.2 (C-aryl), 128.2 (C-aryl), 107.9 (C-29), 81.1 (C-3), 62.8 (-**C**H_2-OAc), 55.6, 53.4, 52.9, 50.4, 49.6, 46.5, 45.1, 42.8, 41.1, 38.6, 38.0, 37.7, 37.2, 34.6, 34.3, 31.6, 29.9, 28.1, 27.2, 26.7, 23.8, 21.5, 21.3, 21.2, 21.1, 18.3, 16.6, 16.3, 16.2, 14.9. IR (DRIFT): 2941.16, 2870.45, 1732.15, 1454.56, 1364.04, 1239.95, 1104.20, 1028.76. HRMS (ASAP, TOF ES$^+$): calcd. for $C_{42}H_{64}NO_4^+$ $[M + H]^+$ 646.4830, found 646.4840.

*4.1.5.8. 3β,28-diacetoxy-30-(4-tert-butylbenzylamino)lup-20(29)-ene (**5h**).* Compound (**5h**) was prepared according to the general procedure for Tsuji-Trost reaction. The reaction time was 24 h. After the column chromatography purification using hexane/EtOAc (1:1) derivative **5h** was obtained in 84% yield as a white solid. $R_f = 0.65$ (hexane/EtOAc 1:1). $[\alpha]_D^{25} = -7.6$ (c = 1.0, THF). ^{1}H NMR (500 MHz, $CDCl_3$): δ 7.37 – 7.33 (m, 2H, aryl), 7.29 – 7.25 (m, 2H, aryl), 4.91 (d, $J = 1.2$ Hz, 1H, H-29), 4.87 (s, 1H, H-29), 4.50 – 4.44 (m, 1H, H-3), 4.24 (dd, $J = 11.2$,

0.9 Hz, 1H, H-28a), 3.83 (d, J = 11.1 Hz, 1H, H-28b), 3.79 (d, J = 13.2 Hz, 1H, part of AB system -CH_2-Ar), 3.75 (d, J = 13.2 Hz, 1H, part of AB system -CH_2-Ar), 3.25 (d, J = 15.0 Hz, 1H, H-30a), 3.18 (d, J = 15.1 Hz, 1H, H-30b), 2.37 (td, J = 10.8, 5.6 Hz, 1H, H-19), 2.06 (s, 3H, CH_3C=O), 2.04 (s, 3H, CH_3C=O), 1.32 (s, 9H, 3 × CH_3), 1.02 (s, 3H, CH_3), 0.92 (s, 3H, CH_3), 0.84 (s, 6H, 2 × CH_3), 0.83 (s, 3H, CH_3). ^{13}C NMR (126 MHz, $CDCl_3$): δ 171.7 (-C=O, ester), 171.1 (-C=O, ester), 152.9 (C-20), 149.9 (C-aryl), 137.6 (C-aryl), 127.9 (C-aryl), 125.4 (C-aryl), 107.9 (C-29), 81.0 (C-3), 62.8 (-**C**H_2-OAc), 55.5, 53.3, 52.9, 50.4, 49.5, 46.4, 45.2, 42.8, 41.1, 38.5, 37.9, 37.6, 37.2, 34.6, 34.6, 34.3, 31.6, 29.9, 28.1, 27.2, 26.6, 23.8, 21.5, 21.2, 21.0, 18.3, 16.6, 16.3, 16.2, 14.9, 14.3. IR (DRIFT): 2945.10, 2870.19, 1732.49, 1456.65, 1389.34, 1363.46, 1238.46, 1106.79, 1028.04. HRMS (ASAP, TOF ES$^+$): calcd. for $C_{45}H_{70}NO_4^+$ $[M + H]^+$ 688.5299, found 688.5313.

*4.1.5.9. 3β,28-diacetoxy-30-(4-fluorobenzylamino)lup-20(29)-ene (**5i**).* Compound (**5i**) was prepared according to the general procedure for Tsuji-Trost reaction. The reaction time was 24 h. After the column chromatography purification using a gradient mobile phase of hexane/EtOAc (6:1 to 3:2) derivative **5i** was obtained in 57% yield as a white solid. R_f = 0.09 (hexane/EtOAc 6:1). $[\alpha]_D^{25}$ = +2.7 (c = 1.0, THF). ^{1}H NMR (500 MHz, $CDCl_3$): δ 7.32 – 7.28 (m, 2H, aryl), 7.03 – 6.98 (m, 2H, aryl), 4.90 (d, J = 1.5 Hz, 1H, H-29), 4.88 (s, 1H, H-29), 4.50 – 4.44 (m, 1H, H-3), 4.23 (dd, J = 11.0, 1.2 Hz, 1H, H-28a), 3.84 (d, J = 10.9 Hz, 1H, H-28b), 3.80 – 3.72 (m, 2H, -CH_2-Ar), 3.22 (d, J = 14.9 Hz, 1H, H-30a), 3.16 (d, J = 14.9 Hz, 1H, H-30b), 2.36 (td, J = 10.4, 5.5 Hz, 1H, H-19), 2.06 (s, 3H, CH_3C=O), 2.04 (s, 3H, CH_3C=O), 1.03 (s, 3H, CH_3), 0.94 (s, 3H, CH_3), 0.84 (s, 6H, 2 × CH_3), 0.83 (s, 3H, CH_3). ^{13}C NMR (126 MHz, $CDCl_3$): δ 171.7 (-C=O, ester), 171.1 (-C=O, ester), 162.1 (d, $^1J_{CF}$ = 244.7 Hz), 152.9 (C-20), 136.4 (d, $^4J_{CF}$ = 3.2 Hz, C-aryl), 129.7 (d, $^3J_{CF}$ = 7.9 Hz, C-aryl), 115.3 (d, $^2J_{CF}$ = 21.2 Hz, C-aryl), 108.0 (C-29), 81.1 (C-3), 62.8 (-**C**H_2-OAc), 55.5, 52.9, 50.4, 49.6, 46.5, 45.1, 42.8, 41.1, 38.6, 38.0, 37.7, 37.2, 34.6, 34.3, 31.6, 29.9, 29.8, 28.1, 27.2, 26.7, 23.8, 21.5, 21.2, 21.1, 18.3, 16.6, 16.3, 16.2, 14.9. IR (DRIFT): 2941.46, 2870.45, 1731.56, 1508.20, 1454.18, 1364.16, 1239.10, 1028.41. HRMS (ASAP, TOF ES$^+$): calcd. for $C_{41}H_{61}FNO_4^+$ $[M + H]^+$ 650.4579, found 650.4596.

*4.1.5.10. 3β,28-diacetoxy-30-(4-chlorobenzylamino)lup-20(29)-ene (**5j**).* Compound (**5j**) was prepared according to the general procedure for Tsuji-Trost reaction. The reaction time was 24 h. After the column chromatography purification using hexane/EtOAc (3:1) derivative **5j** was obtained in 76% yield as a white solid. R_f = 0.23 (hexane/EtOAc 3:1). $[\alpha]_D^{26}$ = −4.4 (c = 1.0, THF). ^{1}H NMR (500 MHz, $CDCl_3$): δ 7.31 – 7.26 (m, 4H, aryl), 4.90 (d, J = 1.1 Hz, 1H, H-29), 4.88 (s, 1H, H-29), 4.50 – 4.43 (m, 1H, H-3), 4.23 (dd, J = 11.1, 0.9 Hz, 1H, H-28a), 3.83 (d, J = 11.1 Hz, 1H, H-28b), 3.78 (d, J = 13.5 Hz, 1H, part of AB system -CH_2-Ar), 3.75 (d, J = 13.5 Hz, 1H, part of AB system -CH_2-Ar), 3.21 (d, J = 14.9 Hz, 1H, H-30a), 3.15 (d, J = 15.0 Hz, 1H, H-30b), 2.42 – 2.29 (m, 1H, H-19), 2.06 (s, 3H, CH_3C=O), 2.04 (s, 3H, CH_3C=O), 1.02 (s, 3H, CH_3), 0.93 (s, 3H, CH_3), 0.84 (s, 6H, 2 × CH_3), 0.83 (s, 3H, CH_3). ^{13}C NMR (126 MHz, $CDCl_3$): δ 171.7 (-C=O, ester), 171.1 (-C=O, ester), 152.8 (C-20), 139.1 (C-aryl), 132.6 (C-aryl), 129.5 (C-aryl), 128.5 (C-aryl), 108.0 (C-29), 81.0 (C-3), 62.7 (-**C**H_2-OAc), 55.4, 52.8, 50.3, 49.5, 46.4, 45.0, 42.7, 41.0, 38.5, 37.9, 37.6, 37.1, 34.5, 34.2, 31.5, 29.8, 28.0, 27.1, 27.0, 26.6, 23.8, 21.4, 21.1, 21.0, 18.2, 16.6, 16.2, 16.1, 14.8. IR (DRIFT): 2942.64, 2866.35, 1731.45, 1456.28, 1388.93, 1363.75, 1239.38, 1088.99, 1028.48, 1014.77. HRMS (ASAP, TOF ES$^+$): calcd. for $C_{41}H_{61}ClNO_4^+$ $[M + H]^+$ 666.4284, found 666.4292.

*4.1.5.11. 3β,28-diacetoxy-30-(4-trifluoromethylbenzyl)aminolup-20(29)-ene (**5k**).* Compound (**5k**) was prepared according to the general procedure for Tsuji-Trost reaction. The reaction time was 24 h. After the column chromatography purification using hexane/EtOAc (3:1) derivative **5k** was obtained in 75% yield as a white solid. R_f = 0.27 (hexane/EtOAc 3:1). $[\alpha]_D^{26}$ = −1.6 (c = 1.0, THF). ^{1}H NMR (500 MHz, $CDCl_3$): δ 7.58 (d, J = 7.9 Hz, 2H, aryl, part of AB system), 7.47 (d, J = 8.0 Hz, 2H, aryl, part of AB system), 4.92 (d, J = 1.4 Hz, 1H, H-29), 4.90 (s, 1H, H-29), 4.49 – 4.44 (m, 1H, H-3), 4.23 (dd, J = 11.1, 1.2 Hz, 1H, H-28a), 3.90 – 3.81 (m, 3H, H-28b, -CH_2-Ar), 3.24 (d, J = 14.9 Hz, 1H, H-30a), 3.18 (d, J = 14.9 Hz, 1H, H-30b), 2.40 – 2.31 (m, 1H, H-19), 2.06 (s, 3H, CH_3C=O), 2.04 (s, 3H, CH_3C=O), 1.02 (s, 3H, CH_3), 0.92 (s, 3H, CH_3), 0.86 – 0.84 (m, 6H, 2 × CH_3), 0.83 (s, 3H, CH_3). ^{13}C NMR (126 MHz, $CDCl_3$): δ 171.7 (-C=O, ester), 171.1 (-C=O, ester), 152.5 (C-20), 144.5, 129.3 (q, $^2J_{CF}$ = 32.2 Hz), 128.5, 126.9 (q, $^1J_{CF}$ = 272.1 Hz), 125.5 (q, $^3J_{CF}$ = 3.6 Hz), 108.3 (C-29), 81.0 (C-3), 62.7 (-**C**H_2-OAc), 55.5, 53.0, 50.4, 49.7, 46.5, 45.0, 42.8, 41.1, 38.5, 37.9, 37.6, 37.2, 34.5, 34.3, 31.6, 29.9, 29.8, 28.1, 27.2, 26.8, 23.8, 21.5, 21.2, 21.0, 18.3, 16.6, 16.3, 16.2, 14.8. IR (DRIFT): 2941.50, 2870.45, 1731.68, 1458.27, 1365.00, 1323.83, 1240.65, 1161.55, 1122.13, 1065.94, 1028.97, 1017.79. HRMS (ASAP, TOF ES$^+$): calcd. for $C_{42}H_{61}F_3NO_4^+$ $[M + H]^+$ 700.4547, found 700.4555.

*4.1.5.12. 3β,28-diacetoxy-30-({[4-(methoxycarbonyl)phenyl]methyl}amino)lup-20(29)-ene (**5l**).* Compound (**5l**) was prepared according to the general procedure for Tsuji-Trost reaction. The reaction time was 24 h. After the column chromatography purification using hexane/EtOAc (1:1) derivative **5l** was obtained in 62% yield as a white solid. R_f = 0.53 (hexane/EtOAc 1:1). $[\alpha]_D^{26}$ = −5.9 (c = 1.0, THF). ^{1}H NMR (500 MHz, $CDCl_3$ δ 8.01 – 7.99 (m, 2H, aryl), 7.43 – 7.40 (m, 2H, aryl), 4.91 (d, J = 1.4 Hz, 1H, H-29), 4.89 (s, 1H, H-29), 4.49 – 4.45 (m, 1H, H-3), 4.23 (dd, J = 11.1, 1.0 Hz, 1H, H-28a), 3.92 (s, 3H, CH_3O), 3.89 – 3.82 (m, 3H, H-28b, -CH_2-Ar), 3.23 (d, J = 14.9 Hz, 1H, H-30a), 3.17 (d, J = 15.0 Hz, 1H, H-30b), 2.36 (dt, J = 15.9, 5.9 Hz, 1H, H-19), 2.06 (s, 3H, CH_3C=O), 2.04 (s, 3H, CH_3C=O), 1.02 (s, 3H, CH_3), 0.92 (s, 3H, CH_3), 0.84 (s, 6H, 2 × CH_3), 0.83 (s, 3H, CH_3). ^{13}C NMR (126 MHz, $CDCl_3$) δ 171.7 (-C=O, ester), 171.1 (-C=O, ester), 167.2 (-**C**(OMe) = O), 152.8 (C-20), 146.1 (C-aryl), 129.9 (C-aryl), 129.0 (C-aryl), 128.0 (C-aryl), 108.2 (C-29), 81.1 (C-3), 62.8 (-**C**H_2-OAc), 55.5, 53.3, 52.9, 52.2, 50.4, 49.6, 46.5, 45.1, 42.8, 41.1, 38.5, 38.0, 37.6, 37.2, 34.6, 34.3, 31.6, 29.9, 28.1, 27.2, 26.7, 23.9, 21.5, 21.2, 21.0, 18.3, 16.6, 16.3, 16.2, 14.9. IR (DRIFT): 2942.83, 2872.49, 1721.57, 1611.77, 1434.87, 1364.24, 1276.35, 1239.36, 1105.41, 1028.32. HRMS (ASAP, TOF ES$^+$): calcd. for $C_{43}H_{64}NO_6^+$ $[M + H]^+$ 690.4728, found 690.4727.

*4.1.5.13. 3β,28-diacetoxy-30-(4-cyanobenzylamino)lup-20(29)-ene (**5m**).* Compound (**5m**) was prepared according to the general procedure for Tsuji-Trost reaction. The reaction time was 24 h. After the column chromatography purification using hexane/EtOAc (2:1) derivative **5m** was obtained in 67% yield as a white solid. R_f = 0.23 (hexane/EtOAc 2:1). $[\alpha]_D^{26}$ = +0.5 (c = 1.0, THF). ^{1}H NMR (500 MHz, $CDCl_3$): δ 7.61 (d, J = 8.1 Hz, 2H, aryl, part of AB system), 7.47 (d, J = 7.9 Hz, 2H, aryl, part of AB system), 4.90 (s, 1H, H-29), 4.89 (s, 1H, H-29), 4.50 – 4.42 (m, 1H, H-3), 4.22 (d, J = 11.1 Hz, 1H, H-28a), 3.90 – 3.79 (m, 3H, H-28b, -CH_2-Ar), 3.22 (d, J = 14.9 Hz, 1H, H-30a), 3.15 (d, J = 14.8 Hz, 1H, H-30b), 2.41 – 2.28 (m, 1H, H-19), 2.06 (s, 3H, CH_3C=O), 2.03 (s, 3H, CH_3C=O), 1.02 (s, 3H, CH_3), 0.93 (s, 3H, CH_3), 0.84 (s, 6H, 2 × CH_3), 0.83 (s, 3H, CH_3). ^{13}C NMR (126 MHz, $CDCl_3$): δ 171.7 (-C=O, ester), 171.1 (-C=O, ester), 152.7 (C-20), 146.3 (C-aryl), 132.3 (C-aryl), 128.7 (C-aryl), 119.1 (-**C**N), 110.9 (C-aryl), 108.3 (C-29), 81.0 (C-3), 62.7 (-**C**H_2-OAc), 55.5, 53.1, 50.4, 49.7, 46.4, 44.9, 42.8, 41.1, 38.5, 37.9, 37.6, 37.2, 34.5, 34.3, 31.7, 29.9, 28.1, 27.2, 26.8, 23.8, 21.4, 21.2, 21.0, 18.3, 16.6, 16.3, 16.2, 14.9. IR (DRIFT): 2942.92, 2870.45, 1730.76, 1456.47, 1389.21, 1363.94, 1239.74, 1028.68. HRMS (ASAP, TOF ES$^+$): calcd. for $C_{42}H_{61}N_2O_4^+$ $[M + H]^+$ 657.4626; found 657.4633.

*4.1.5.14. 3β,28-diacetoxy-30-(4-methoxybenzylamino)lup-20(29)-ene (**5n**).* Compound (**5n**) was prepared according to the general procedure for Tsuji-Trost reaction. The reaction time was 24 h. After the column chromatography purification using a gradient mobile phase of hexane/

EtOAc (6:1 to 3:2) derivative **5n** was obtained in 85% yield as a white solid. R_f = 0.06 (hexane/EtOAc 6:1). $[\alpha]_D^{23}$ = −5.6 (c = 1.0, THF). ^{1}H NMR (500 MHz, $CDCl_3$): δ 7.27 – 7.23 (m, 2H, aryl), 6.88 – 6.84 (m, 2H, aryl), 4.89 (d, *J* = 1.5 Hz, 1H, H-29), 4.87 (s, 1H, H-29), 4.50 – 4.44 (m, 1H, H-3), 4.24 (dd, *J* = 11.1, 1.1 Hz, 1H, H-28a), 3.83 (d, *J* = 11.1 Hz, 1H, H-28b), 3.81 (s, 3H, CH_3O), 3.75 (d, *J* = 13.0 Hz, 1H, -CH_2-Ar, part of AB system), 3.71 (d, *J* = 13.0 Hz, 1H, -CH_2-Ar, part of AB system), 3.22 (d, *J* = 15.0 Hz, 1H, H-30a), 3.16 (d, *J* = 14.9 Hz, 1H, H-30b), 2.40 – 2.31 (m, 1H, H-19), 2.06 (s, 3H, CH_3C=O), 2.04 (s, 3H, CH_3C=O), 1.02 (s, 3H, CH_3), 0.93 (s, 3H, CH_3), 0.84 (s, 6H, 2 × CH_3), 0.83 (s, 3H, CH_3). ^{13}C NMR (126 MHz, $CDCl_3$): δ 171.7 (-C=O, ester), 171.1 (-C=O, ester), 158.8 (C-aryl), 152.9 (C-20), 132.8 (C-aryl), 129.4 (C-aryl), 113.9 (C-aryl), 107.9 (C-29), 81.1 (C-3), 62.8 (-**C**H_2-OAc), 55.5, 55.4, 53.1, 52.9, 50.4, 49.5, 46.4, 45.1, 42.8, 41.1, 38.5, 37.9, 37.6, 37.2, 34.5, 34.3, 31.6, 29.9, 28.1, 27.2, 26.6, 23.8, 21.5, 21.2, 21.0, 18.3, 16.6, 16.3, 16.2, 14.9. IR (DRIFT): 2941.83, 2864.31, 1731.21, 1511.28, 1455.49, 1363.76, 1239.54, 1102.16, 1029.18. HRMS (ASAP, TOF ES$^+$): calcd. for $C_{42}H_{64}NO_5^+$ [M + H]$^+$ 662.4779; found 662.4778.

*4.1.5.15. 3β,28-diacetoxy-30-(4-methylthiobenzylamino)lup-20(29)-ene (**5o**).* Compound (**5o**) was prepared according to the general procedure for Tsuji-Trost reaction. The reaction time was 24 h. After the column chromatography purification using hexane/EtOAc (1:1) derivative **5o** was obtained in 69% yield as a white solid. R_f = 0.43 (hexane/EtOAc 1:1). $[\alpha]_D^{26}$ = −1.3 (c = 1.0, THF). ^{1}H NMR (500 MHz, $CDCl_3$): δ 7.27 – 7.22 (m, 4H, aryl), 4.90 (d, *J* = 1.3 Hz, 1H, H-29), 4.87 (s, 1H, H-29), 4.49 – 4.45 (m, 1H, H-3), 4.23 (dd, *J* = 11.1, 1.2 Hz, 1H, H-28a), 3.83 (d, *J* = 11.0 Hz, 1H, H-28b), 3.78 (d, *J* = 13.3 Hz, 1H, -CH_2-Ar, part of AB system), 3.74 (d, *J* = 13.3 Hz, 1H, -CH_2-Ar, part of AB system), 3.22 (d, *J* = 14.9 Hz, 1H, H-30a), 3.16 (d, *J* = 15.0 Hz, 1H, H-30b), 2.48 (s, 3H, CH_3S), 2.40 – 2.31 (m, 1H, H-19), 2.06 (s, 3H, CH_3C=O), 2.04 (s, 3H, CH_3C=O), 1.02 (s, 3H, CH_3), 0.93 (s, 3H, CH_3), 0.84 (s, 6H, 2 × CH_3), 0.83 (s, 3H, CH_3). ^{13}C NMR (126 MHz, $CDCl_3$): δ 171.7 (-C=O, ester), 171.1 (-C=O, ester), 152.9 (C-20), 137.7 (C-aryl), 136.9 (C-aryl), 128.8 (C-aryl), 127.1 (C-aryl), 108.0 (C-29), 81.1 (C-3), 62.8 (-**C**H_2-OAc), 55.5, 53.2, 52.8, 50.4, 49.6, 46.4, 45.1, 42.8, 41.1, 38.5, 38.0, 37.7, 37.2, 34.6, 34.3, 31.6, 31.1, 29.9, 28.1, 27.2, 26.7, 23.8, 21.5, 21.2, 21.1, 18.3, 16.6, 16.3, 16.2, 14.9. IR (DRIFT): 2941.18, 2864.31, 1730.75, 1458.27, 1363.36, 1239.36, 1027.94. HRMS (ASAP, TOF ES$^+$): calcd. for $C_{42}H_{64}NO_4S^+$ [M + H]$^+$ 678.4551, found 678.4568.

*4.1.5.16. 3β,28-diacetoxy-30-(4-ethoxybenzylamino)lup-20(29)-ene (**5p**).* Compound (**5p**) was prepared according to the general procedure for Tsuji-Trost reaction. The reaction time was 24 h. After the column chromatography purification using hexane/EtOAc (3:2) derivative **5p** was obtained in 68% yield as a white solid. R_f = 0.22 (hexane/EtOAc 3:2). $[\alpha]_D^{26}$ = −10.5 (c = 1.0, THF). ^{1}H NMR (500 MHz, $CDCl_3$): δ 7.25 – 7.22 (m, 2H, aryl), 6.87 – 6.83 (m, 2H, aryl), 4.89 (d, *J* = 1.2 Hz, 1H, H-29), 4.87 (s, 1H, H-29), 4.49 – 4.44 (m, 1H, H-3), 4.24 (dd, *J* = 11.1, 1.0 Hz, 1H, H-28a), 4.03 (q, *J* = 7.0 Hz, 2H, CH_3**C**H_2O-), 3.83 (d, *J* = 11.0 Hz, 1H, H-28b), 3.75 (d, *J* = 13.0 Hz, 1H, -CH_2-Ar, part of AB system), 3.71 (d, *J* = 12.9 Hz, 1H, -CH_2-Ar, part of AB system), 3.22 (d, *J* = 15.0 Hz, 1H, H-30a), 3.15 (d, *J* = 15.0 Hz, 1H, H-30b), 2.40 – 2.29 (m, 1H, H-19), 2.06 (s, 3H, CH_3C=O), 2.04 (s, 3H, CH_3C=O), 1.41 (t, *J* = 7.0 Hz, 3H, C**H**$_3$$CH_2$O-), 1.02 (s, 3H, CH_3), 0.93 (s, 3H, CH_3), 0.84 (s, 6H, 2 × CH_3), 0.83 (s, 3H, CH_3). ^{13}C NMR (126 MHz, $CDCl_3$): δ 171.7 (-C=O, ester), 171.1 (-C=O, ester), 158.1 (C-aryl), 152.9 (C-20), 132.6 (C-aryl), 129.4 (C-aryl), 114.5 (C-aryl), 107.8 (C-29), 81.0 (C-3), 63.6, 62.8 (-**C**H_2-OAc), 55.5, 53.1, 52.8, 50.4, 49.5, 46.4, 45.1, 42.8, 41.1, 38.5, 37.9, 37.6, 37.2, 34.5, 34.3, 31.6, 29.9, 28.1, 27.2, 26.6, 23.8, 21.5, 21.2, 21.0, 18.3, 16.6, 16.3, 16.2, 15.0, 14.9. IR (DRIFT): 2940.44, 2868.40, 1731.44, 1510.22, 1455.78, 1389.69; 1363.80, 1236.15, 1172.19, 1114.88, 1028.38. HRMS (ASAP, TOF ES$^+$): calcd. for $C_{43}H_{66}NO_5^+$ [M + H]$^+$ 676.4936, found 676.4944.

*4.1.5.17. 3β,28-diacetoxy-30-(2,4-dimethoxybenzylamino)lup-20(29)-ene (**5q**).* Compound (**5q**) was prepared according to the general procedure for Tsuji-Trost reaction. The reaction time was 24 h. After the column chromatography purification using a gradient mobile phase of hexane/EtOAc (1:1 to 0:1) derivative **5q** was obtained in 67% yield as a white solid. R_f = 0.36 (EtOAc). $[\alpha]_D^{26}$ = −1.3 (c = 1.0, THF). ^{1}H NMR (500 MHz, $CDCl_3$): δ 7.14 (d, *J* = 8.1 Hz, 1H, aryl), 6.46 – 6.42 (m, 2H, aryl), 4.90 (d, *J* = 1.2 Hz, 1H, H-29), 4.85 (s, 1H, H-29), 4.49 – 4.45 (m, 1H, H-3), 4.23 (dd, *J* = 11.0, 1.1 Hz, 1H. H-28a), 3.83 (d, *J* = 11.2 Hz, 1H, H-28b), 3.81 (s, 6H, 2 × CH_3O), 3.76 (d, *J* = 13.3 Hz, 1H, -CH_2-Ar, part of AB system), 3.69 (d, *J* = 13.3 Hz, 1H, -CH_2-Ar, part of AB system), 3.19 (d, *J* = 15.2 Hz, 1H, H-30a), 3.13 (d, *J* = 15.2 Hz, 1H, H-30b), 2.35 (dt, *J* = 15.8, 5.5 Hz, 1H, H-19), 2.06 (s, 3H, CH_3C=O), 2.04 (s, 3H, CH_3C=O), 1.02 (s, 3H, CH_3), 0.92 (s, 3H, CH_3), 0.86 – 0.84 (m, 6H, 2 × CH_3), 0.83 (s, 3H, CH_3). ^{13}C NMR (126 MHz, $CDCl_3$): δ 171.7 (-C=O, ester), 171.1 (-C=O, ester), 160.2 (C-aryl), 158.8 (C-aryl), 153.0 (C-20), 130.5 (C-aryl), 121.2 (C-aryl), 107.7 (C-29), 103.8 (C-aryl), 98.7 (C-aryl), 81.1 (C-3), 62.8 (-**C**H_2-OAc), 55.6, 55.5, 55.4, 52.4, 50.4, 49.5, 48.6, 46.4, 45.2, 42.8, 41.1, 38.5, 38.0, 37.7, 37.2, 34.5, 34.3, 31.4, 29.9, 28.1, 27.2, 26.5, 23.9, 21.5, 21.2, 21.1, 18.3, 16.6, 16.3, 16.2, 14.9. IR (DRIFT): 2940.51, 2866.35, 1730.77, 1611.77, 1587.21, 1503.30, 1455.43, 1363.91, 1286.96, 1239.39, 1206.61, 1155.11, 1130.39, 1029.24. HRMS (ASAP, TOF ES$^+$): calcd. for $C_{43}H_{66}NO_6^+$ [M + H]$^+$ 692.4885, found 692.4893.

*4.1.5.18. 3β,28-diacetoxy-30-{[2-(4-methoxyphenyl)ethyl]amino}lup-20(29)-ene (**5r**).* Compound (**5r**) was prepared according to the general procedure for Tsuji-Trost reaction. The reaction time was 24 h. After the column chromatography purification using EtOAc derivative **5r** was obtained in 80% yield as a white solid. R_f = 0.34 (EtOAc). $[\alpha]_D^{26}$ = +0.2 (c = 1.0, THF). ^{1}H NMR (500 MHz, $CDCl_3$): δ 7.15 – 7.11 (m, 2H, aryl), 6.86 – 6.82 (m, 2H, aryl), 4.82 (s, 1H, H-29), 4.78 (d, *J* = 1.0 Hz, 1H, H-29), 4.50 – 4.43 (m, 1H, H-3), 4.23 (dd, *J* = 11.2, 0.8 Hz, 1H, H-28a), 3.82 (d, *J* = 11.0 Hz, 1H, H-28b), 3.79 (s, 3H, CH_3O), 3.21 (d, *J* = 15.3 Hz, 1H, H-30a), 3.14 (d, *J* = 15.2 Hz, 1H, H-30b), 2.89 – 2.73 (m, 4H), 2.38 – 2.24 (m, 1H, H-19), 2.06 (s, 3H, CH_3C=O), 2.04 (s, 3H, CH_3C=O), 1.02 (s, 3H, CH_3), 0.95 (s, 3H, CH_3), 0.84 (s, 6H, 2 × CH_3), 0.83 (s, 3H, CH_3). ^{13}C NMR (126 MHz, $CDCl_3$): δ 171.7 (-C=O, ester), 171.1 (-C=O, ester), 158.2 (C-aryl), 152.8 (C-20), 132.3 (C-aryl), 129.8 (C-aryl), 114.0 (C-aryl), 107.5 (C-29), 81.0 (C-3), 62.7 (-**C**H_2-OAc), 55.5, 55.4, 53.3, 51.2, 50.4, 49.5, 46.4, 45.1, 42.8, 41.1, 38.5, 37.9, 37.6, 37.2, 35.7, 34.6, 34.3, 31.5, 29.9, 28.1, 27.2, 26.7, 23.8, 21.5, 21.2, 21.0, 18.3, 16.6, 16.3, 16.2, 14.9. IR (DRIFT): 2940.90, 2870.45, 1730.94, 1511.91, 1455.90, 1363.93, 1239.55, 1176.09, 1029.18. HRMS (ASAP, TOF ES$^+$): calcd. for $C_{43}H_{66}NO_5^+$ [M + H]$^+$ 676.4936; found 676.4939.

*4.1.5.19. 3β,28-diacetoxy-30-(4-hydroxybenzylamino)lup-20(29)-ene (**5s**).* Compound (**5s**) was prepared according to the general procedure for Tsuji-Trost reaction. The reaction time was 24 h. After the column chromatography purification using EtOAc derivative **5s** was obtained in 81% yield as a white solid. R_f = 0.41 (EtOAc). $[\alpha]_D^{26}$ = −3.6 (c = 1.0, THF). ^{1}H NMR (500 MHz, $CDCl_3$): δ 7.17 – 7.12 (m, 2H, aryl), 6.75 – 6.70 (m, 2H, aryl), 4.89 (s, 2H, 2 × H-29), 4.50 – 4.43 (m, 1H, H-3), 4.22 (d, *J* = 11.1 Hz, 1H, H-28a), 3.82 (d, *J* = 11.2 Hz, 1H, H-28b), 3.73 (d, *J* = 12.8 Hz, 1H, -CH_2-Ar, part of AB system), 3.69 (d, *J* = 12.8 Hz, 1H, -CH_2-Ar, part of AB system), 3.26 (d, *J* = 15.2 Hz, 1H, H-30a), 3.18 (d, *J* = 15.1 Hz, 1H, H-30b), 2.31 (td, *J* = 10.8, 5.4 Hz, 1H, H-19), 2.07 (s, 3H, CH_3C=O), 2.04 (s, 3H, CH_3C=O), 1.01 (s, 3H, CH_3), 0.93 (s, 3H, CH_3), 0.84 (s, 3H, CH_3), 0.84 (s, 3H, CH_3), 0.83 (s, 3H, CH_3). ^{13}C NMR (126 MHz, $CDCl_3$): δ 171.9 (-C=O, ester), 171.3 (-C=O, ester), 155.5 (C-aryl), 152.4 (C-20), 131.6 (C-aryl), 129.8 (C-aryl), 115.7 (C-aryl), 108.2 (C-29), 81.2 (C-3), 62.8 (-**C**H_2-OAc), 55.5, 53.1, 52.7, 50.4, 49.7, 46.4, 45.0, 42.8, 41.0, 38.5, 37.9, 37.6, 37.2, 34.5, 34.3, 31.6, 29.9, 28.1, 27.2, 26.7, 23.8, 21.5, 21.2, 21.0, 18.3, 16.6, 16.3, 16.2, 14.9. IR

(DRIFT): 2941.36, 2870.45, 1732.12, 1515.23, 1455.80, 1364.34, 1240.04, 1029.01. HRMS (ASAP, TOF ES$^+$): calcd. for $C_{41}H_{62}NO_5^+$ [M + H]$^+$ 648.4623, found 648.4633.

*4.1.5.20. 3β,28-diacetoxy-30-(4-dimethylaminobenzylamino)lup-20(29)-ene (**5t**).* Compound (**5t**) was prepared according to the general procedure for Tsuji-Trost reaction. The reaction time was 24 h. After the column chromatography purification using EtOAc derivative **5t** was obtained in 77% yield as a white solid. $R_f = 0.38$ (EtOAc). $[\alpha]_D^{26} = -7.2$ (c = 1.0, THF). ^{1}H NMR (500 MHz, $CDCl_3$): δ 7.22 – 7.18 (m, 2H, aryl), 6.73 – 6.70 (m, 2H, aryl), 4.89 (d, *J* = 1.2 Hz, 1H, H-29), 4.86 (s, 1H, H-29), 4.50 – 4.43 (m, 1H, H-3), 4.24 (dd, *J* = 11.0, 1.0 Hz, 1H, H-28a), 3.83 (d, *J* = 10.9 Hz, 1H, H-28b), 3.73 (d, *J* = 12.9 Hz, 1H, -CH_2-Ar, part of AB system), 3.68 (d, *J* = 12.8 Hz, 1H, -CH_2-Ar, part of AB system), 3.23 (d, *J* = 15.1 Hz, 1H, H-30a), 3.16 (d, *J* = 15.0 Hz, 1H, H-30b), 2.94 (s, 6H, 2 × CH_3), 2.36 (td, *J* = 9.5, 4.2 Hz, 1H, H-19), 2.06 (s, 3H, CH_3C=O), 2.04 (s, 3H, CH_3C=O), 1.02 (s, 3H, CH_3), 0.93 (s, 3H, CH_3), 0.86 – 0.84 (m, 6H, 2 × CH_3), 0.83 (s, 3H, CH_3). ^{13}C NMR (126 MHz, $CDCl_3$): δ 171.7 (-C=O, ester), 171.1 (-C=O, ester), 152.9 (C-20), 150.0 (C-aryl), 129.2 (C-aryl), 128.6 (C-aryl), 112.9 (C-aryl), 107.8 (C-29), 81.1 (C-3), 62.8 (-**C**H_2-OAc), 55.5, 53.2, 52.5, 50.4, 49.5, 46.4, 45.2, 42.8, 41.0, 40.9, 38.5, 37.9, 37.6, 37.2, 34.5, 34.3, 31.5, 29.9, 28.1, 27.2, 26.6, 23.8, 21.5, 21.2, 21.0, 18.3, 16.6, 16.3, 16.2, 14.9. IR (DRIFT): 2941.69, 2870.45, 1731.68, 1613.82, 1521.47, 1456.01, 1388.98, 1363.30, 1239.30, 1164.02, 1028.08. HRMS (ASAP, TOF ES$^+$): calcd. for $C_{43}H_{67}N_2O_4^+$ [M + H]$^+$ 675.5095, found 675.5098.

*4.1.5.21. 3β,28-diacetoxy-30-[(pyridin-4-ylmethyl)amino]lup-20(29)-ene (**5u**).* Compound (**5u**) was prepared according to the general procedure for Tsuji-Trost reaction. The reaction time was 24 h. After the column chromatography purification using a gradient mobile phase of hexane/EtOAc (1:1 to 0:1) derivative **5u** was obtained in 80% yield as a white solid. $R_f = 0.22$ (EtOAc). $[\alpha]_D^{25} = -5.1$ (c = 1.0, THF). ^{1}H NMR (500 MHz, $CDCl_3$): δ 8.58 – 8.50 (m, 2H, aryl), 7.31 – 7.23 (m, 2H, aryl), 4.91 (s, 1H, H-29), 4.90 (s, 1H, H-29), 4.50 – 4.41 (m, 1H, H-3), 4.23 (d, *J* = 11.0 Hz, 1H, H-28a), 3.87 – 3.77 (m, 3H, H-28b, -CH_2-Ar), 3.22 (d, *J* = 14.9 Hz, 1H, H-30a), 3.16 (d, *J* = 14.9 Hz, 1H, H-30b), 2.42 – 2.30 (m, 1H, H-19), 2.06 (s, 3H, CH_3C=O), 2.03 (s, 3H, CH_3C=O), 1.02 (s, 3H, CH_3), 0.93 (s, 3H, CH_3), 0.86 – 0.80 (m, 9H, 3 × CH_3). ^{13}C NMR (126 MHz, $CDCl_3$): δ 171.7 (-C=O, ester), 171.1 (-C=O, ester), 152.7 (C-20), 150.0 (C-aryl), 149.7 (C-aryl), 123.0 (C-aryl), 108.3 (C-29), 81.0 (C-3), 62.7 (-**C**H_2-OAc), 55.5, 53.1, 52.3, 50.4, 49.7, 46.5, 44.9, 42.8, 41.1, 38.5, 37.9, 37.6, 37.2, 34.5, 34.3, 31.7, 29.9, 28.1, 27.2, 26.8, 23.8, 21.4, 21.2, 21.0, 18.3, 16.6, 16.3, 16.2, 14.9. IR (DRIFT): 2940.51, 2868.40, 1730.72, 1599.49, 1456.23, 1363.64, 1238.57, 1028.31. HRMS (ASAP, TOF ES$^+$): calcd. for $C_{40}H_{61}N_2O_4^+$ [M + H]$^+$ 633.4626, found 633.4638.

*4.1.5.22. 3β,28-diacetoxy-30-[(thiophen-2-ylmethyl)amino]lup-20(29)-ene (**5v**).* Compound (**5v**) was prepared according to the general procedure for Tsuji-Trost reaction. The reaction time was 24 h. After the column chromatography purification using a gradient mobile phase of hexane/EtOAc (6:1 to 1:1) derivative **5v** was obtained in 93% yield as a white solid. $R_f = 0.86$ (hexane/EtOAc 1:1). $[\alpha]_D^{25} = -2.1$ (c = 1.0, THF). ^{1}H NMR (500 MHz, $CDCl_3$): δ 7.21 (dd, *J* = 5.0, 1.3 Hz, 1H, aryl, part of ABX system), 6.95 (dd, *J* = 5.1, 3.4 Hz, 1H, aryl, part of ABX system), 6.93 – 6.91 (m, 1H, aryl), 4.90 (d, *J* = 1.5 Hz, 1H, H-29), 4.88 (s, 1H, H-29), 4.49 – 4.45 (m, 1H, H-3), 4.24 (dd, *J* = 11.1, 1.3 Hz, 1H, H-28a), 4.01 (dd, *J* = 14.0, 0.9 Hz, 1H, -CH_2-Ar, part of ABX system), 3.97 (dd, *J* = 14.0, 0.9 Hz, 1H, -CH_2-Ar, part of AB system), 3.83 (d, *J* = 10.9 Hz, 1H, H-28b), 3.27 (d, *J* = 14.9 Hz, 1H, H-30a), 3.20 (d, *J* = 14.8 Hz, 1H, H-30b), 2.37 (td, *J* = 11.1, 5.6 Hz, 1H, H-19), 2.06 (s, 3H, CH_3C=O), 2.04 (s, 3H, CH_3C=O), 1.03 (s, 3H, CH_3), 0.94 (s, 3H, CH_3), 0.84 (s, 6H, 2 × CH_3), 0.83 (s, 3H, CH_3). ^{13}C NMR (126 MHz, $CDCl_3$): δ 171.7 (-C=O, ester), 171.1 (-C=O, ester), 152.6 (C-20), 144.5 (C-aryl), 126.7 (C-aryl), 124.9 (C-aryl), 124.5 (C-aryl), 108.3 (C-29), 81.1 (C-3), 62.8 (-**C**H_2-OAc), 55.5, 52.5, 50.4, 49.5, 48.1, 46.5, 45.1, 42.8, 41.1, 38.6, 38.0, 37.6, 37.2, 34.5, 34.3, 31.6, 29.9, 28.1, 27.2, 26.6, 23.8, 21.4, 21.2, 21.1, 18.3, 16.6, 16.3, 16.2, 14.9. IR (DRIFT): 2940.64, 2868.40, 1731.21, 1454.86, 1389.00, 1363.85, 1238.69, 1028.35. HRMS (ASAP, TOF ES$^+$): calcd. for $C_{39}H_{60}NO_4S^+$ [M + H]$^+$ 638.4238, found 638.4250.

*4.1.5.23. 3β,28-diacetoxy-30-[(furane-2-ylmethyl)amino]lup-20(29)-ene (**5w**).* Compound (**5w**) was prepared according to the general procedure for Tsuji-Trost reaction. The reaction time was 24 h. After the column chromatography purification using a gradient mobile phase of hexane/EtOAc (6:1 to 3:2) derivative **5w** was obtained in 84% yield as a white solid. $R_f = 0.11$ (hexane/EtOAc 6:1). $[\alpha]_D^{25} = -3.7$ (c = 1.0, THF). ^{1}H NMR (500 MHz, $CDCl_3$): δ 7.36 (dd, *J* = 1.8, 0.9 Hz, 1H, aryl, part of ABX system), 6.32 (dd, *J* = 3.2, 1.9 Hz, 1H, aryl, part of ABX system), 6.17 (dd, *J* = 3.2, 0.8 Hz, 1H, aryl, part of ABX system), 4.88 – 4.86 (m, 2H, H-29), 4.49 – 4.44 (m, 1H, H-3), 4.23 (dd, *J* = 11.1, 1.2 Hz, 1H, H-28a), 3.84 – 3.74 (m, 3H, H-28b, -CH_2-Ar), 3.21 (d, *J* = 15.0 Hz, 1H, H-30a), 3.14 (d, *J* = 15.0 Hz, 1H, H-30b), 2.40 – 2.29 (m, 1H, H-19), 2.06 (s, 3H, CH_3C=O), 2.03 (s, 3H, CH_3C=O), 1.02 (s, 3H, CH_3), 0.94 (s, 3H, CH_3), 0.84 (s, 6H, 2 × CH_3), 0.83 (s, 3H, CH_3). ^{13}C NMR (126 MHz, $CDCl_3$): δ 171.7 (-C=O, ester), 171.1 (-C=O, ester), 154.2 (C-aryl), 152.5 (C-20), 141.9 (C-aryl), 110.2 (C-aryl), 108.0 (C-29), 107.0 (C-aryl), 81.0 (C-3), 62.7 (-**C**H_2-OAc), 55.5, 52.3, 50.4, 49.5, 46.4, 45.8, 45.1, 42.8, 41.1, 38.5, 37.9, 37.6, 37.2, 34.5, 34.3, 31.5, 29.9, 28.1, 27.2, 26.6, 23.8, 21.5, 21.2, 21.0, 18.3, 16.6, 16.3, 16.2, 14.8. IR (DRIFT): 2941.36, 2870.45, 1731.35, 1458.27, 1364.20, 1239.53, 1151.28, 1028.51. HRMS (ASAP, TOF ES$^+$): calcd. for $C_{39}H_{60}NO_5^+$ [M + H]$^+$ 622.4466, found 622.4465.

*4.1.5.24. 3β,28-diacetoxy-30-[(pyrimidin-2-ylmethyl)amino]lup-20(29)-ene (**5x**).* Compound (**5x**) was prepared according to the general procedure for Tsuji-Trost reaction. The reaction time was 24 h. After the column chromatography purification using EtOAc/MeOH (15:1) derivative **5x** was obtained in 61% yield as a white solid. $R_f = 0.25$ (EtOAc/MeOH 15:1). $[\alpha]_D^{25} = -10.5$ (c = 1.0, THF). ^{1}H NMR (500 MHz, $CDCl_3$): δ 8.71 (d, *J* = 4.9 Hz, 2H, aryl), 7.18 (t, *J* = 4.9 Hz, 1H, aryl), 4.95 (d, *J* = 1.1 Hz, 1H, H-29), 4.90 (s, 1H, H-29), 4.50 – 4.44 (m, 1H, H-3), 4.24 (dd, *J* = 11.1, 1.0 Hz, 1H, H-28a), 4.10 (d, *J* = 15.9 Hz, 1H, -CH_2-Ar, part of AB system), 4.06 (d, *J* = 15.9 Hz, 1H, -CH_2-Ar, part of AB system), 3.83 (d, *J* = 11.0 Hz, 1H, H-28b), 3.31 (d, *J* = 15.0 Hz, 1H, H-30a), 3.23 (d, *J* = 15.1 Hz, 1H, H-30b), 2.43 – 2.33 (m, 1H, H-19), 2.06 (s, 3H, CH_3C=O), 2.04 (s, 3H, CH_3C=O), 1.02 (s, 3H, CH_3), 0.93 (s, 3H, CH_3), 0.84 (s, 6H, 2 × CH_3), 0.83 (s, 3H, CH_3). ^{13}C NMR (126 MHz, $CDCl_3$): δ 171.7 (-C=O, ester), 171.1 (-C=O, ester), 169.3 (C-aryl), 157.2 (C-aryl), 152.5 (C-20), 119.3 (C-aryl), 108.1 (C-29), 81.1 (C-3), 62.8 (-**C**H_2-OAc), 55.5, 55.2, 52.7, 50.4, 49.6, 46.5, 45.1, 42.8, 41.1, 38.6, 38.0, 37.6, 37.2, 34.6, 34.3, 31.4, 29.9, 28.1, 27.2, 26.6, 23.9, 21.5, 21.2, 21.0, 18.3, 16.6, 16.3, 16.2, 14.9. IR (DRIFT): 2941.82, 2872.49, 1730.99, 1561.52, 1422.56, 1389.51, 1364.48, 1239.46, 1029.17. HRMS (ASAP, TOF ES$^+$): calcd. for $C_{39}H_{60}N_3O_4^+$ [M + H]$^+$ 634.4578, found 634.4578.

*4.1.6. Synthesis of tertiary amines **6a** and **6b***

*4.1.6.1. 3β,28-diacetoxy-30-[benzyl(methyl)amino]lup-20(29)-ene (**6a**).* Compound (**6a**) was prepared according to the general procedure for Tsuji-Trost reaction. The reaction time was 24 h. After the column chromatography purification using hexane/EtOAc (6:1) derivative **6a** was obtained in 90% yield as a white solid. $R_f = 0.38$ (hexane/EtOAc 6:1). $[\alpha]_D^{25} = -2.8$ (c = 1.0, THF). ^{1}H NMR (400 MHz, $CDCl_3$): δ 7.36 – 7.27 (m, 4H, aryl), 7.25 – 7.20 (m, 1H, aryl), 4.99 (d, *J* = 1.1 Hz, 1H, H-29), 4.89 (d, *J* = 1.0 Hz, 1H, H-29), 4.50 – 4.44 (m, 1H, H-3), 4.25 (dd, *J* = 11.1, 1.9 Hz, 1H, H-28a), 3.83 (d, *J* = 11.0 Hz, 1H, H-28b), 3.52 (d, *J* = 13.2 Hz, 1H, -CH_2-Ph, part of AB system), 3.45 (d, *J* = 13.2 Hz, 1H, -CH_2-Ph, part of AB system), 2.90 (d, *J* = 14.3 Hz, 1H, H-30a), 2.85 (d, *J* = 14.2 Hz, 1H, H-30b), 2.40 (td, *J* = 10.3, 5.5 Hz, 1H, H-19), 2.17 (s,

3H, CH_3N-), 2.07 (s, 3H, CH_3C=O), 2.04 (s, 3H, CH_3C=O), 1.02 (s, 3H, CH_3), 0.89 (s, 3H, CH_3), 0.84 (s, 3H, CH_3), 0.84 – 0.82 (m, 6H, 2 × CH3). ^{13}C NMR (101 MHz, $CDCl_3$): δ 171.7 (-C=O, ester), 171.1 (-C=O, ester), 151.8 (C-20), 139.8 (C-aryl), 128.9 (C-aryl), 128.3 (C-aryl), 127.0 (C-aryl), 110.0 (C-29), 81.1 (C-3), 77.4, 62.9 (-**C**H_2-OAc), 62.5, 55.5, 50.4, 49.6, 46.4, 44.7, 42.9, 42.8, 41.0, 38.6, 38.0, 37.6, 37.2, 34.5, 34.3, 31.3, 29.9, 28.1, 27.2, 26.6, 23.9, 21.5, 21.2, 21.1, 18.3, 16.6, 16.3, 16.2, 14.8. IR (DRIFT): 2941.65, 2874.54, 2788.58, 1732.26, 1454.70, 1363.94, 1239.54, 1027.49. HRMS (ASAP, TOF ES+): calcd. for $C_{42}H_{64}NO_4^+$ $[M + H]^+$ 646.4830, found 646.4846.

*4.1.6.2. 3β,28-diacetoxy-30-[(4-methoxybenzyl)(methyl)amino]lup-20 (29)-ene (**6b**).* Compound (**6b**) was prepared according to the general procedure for Tsuji-Trost reaction. The reaction time was 24 h. After the column chromatography purification using hexane/EtOAc (6:1) derivative **6b** was obtained in 82% yield as a white solid. R_f = 0.33 (hexane/EtOAc 6:1). ^{1}H NMR (500 MHz, $CDCl_3$): δ 7.25 – 7.22 (m, 2H, aryl), 6.87 – 6.84 (m, 2H, aryl), 4.96 (d, *J* = 1.0 Hz, 1H, H-29), 4.88 (d, *J* = 1.0 Hz, 1H, H-29), 4.49 – 4.44 (m, 1H, H-3), 4.25 (dd, *J* = 11.1, 0.9 Hz, 1H, H-28a), 3.83 (d, *J* = 11.1 Hz, 1H, H-28b), 3.80 (s, 3H, CH_3O), 3.44 (d, *J* = 13.0 Hz, 1H, -CH_2-Ar, part of AB system), 3.39 (d, *J* = 12.9 Hz, 1H, -CH_2-Ar, part of AB system), 2.87 (d, *J* = 14.2 Hz, 1H, H-30a), 2.83 (d, *J* = 14.2 Hz, 1H, H-30b), 2.39 (dt, *J* = 15.5, 5.2 Hz, 1H, H-19), 2.15 (s, 3H, CH_3N-), 2.07 (s, 3H, CH_3C=O), 2.04 (s, 3H, CH_3C=O), 1.02 (s, 3H, CH_3), 0.89 (s, 3H, CH_3), 0.84 (s, 3H, CH_3), 0.84 (s, 3H, CH_3), 0.83 (s, 3H, CH_3). ^{13}C NMR (126 MHz, $CDCl_3$): δ 171.7 (-C=O, ester), 171.1 (-C=O, ester), 158.7 (C-aryl), 152.1 (C-20), 131.9 (C-aryl), 130.1 (C-aryl), 113.7 (C-aryl), 110.0 (C-29), 81.1 (C-3), 62.9 (-**C**H_2-OAc), 61.9, 55.6, 55.4, 50.4, 49.6, 46.4, 44.6, 42.8, 42.8, 41.1, 38.5, 38.0, 37.7, 37.2, 34.5, 34.3, 31.4, 31.1, 29.9, 28.1, 27.2, 26.6, 23.9, 21.5, 21.2, 21.1, 18.3, 16.6, 16.3, 16.2, 14.9. IR (DRIFT): 2941.46, 2868.40, 1732.07, 1609.72, 1510.75, 1454.18, 1364.06, 1239.12, 1028.31. HRMS (ASAP, TOF ES$^+$): calcd. for $C_{43}H_{66}NO_5^+$ $[M + H]^+$ 676.4936, found 676.4940.

*4.1.7. Synthesis of tertiary amines **7a-7e** with cyclic moiety*

*4.1.7.1. 3β,28-diacetoxy-30-(pyrrolidin-1-yl)lup-20(29)-ene (**7a**).* Compound (**7a**) was prepared according to the general procedure for Tsuji-Trost reaction. The reaction time was 24 h. After the column chromatography purification using a gradient mobile phase of hexane/EtOAc (6:1 to 0:1) derivative **7a** was obtained in 79% yield as a white solid. R_f = 0.20 (EtOAc). $[\alpha]_D^{25}$ = + 2.3 (c = 1.0, THF). ^{1}H NMR (500 MHz, $CDCl_3$): δ 4.89 (d, *J* = 1.1 Hz, 1H, H-29), 4.85 (s, 1H, H-29), 4.50 – 4.44 (m, 1H, H-3), 4.25 (dd, *J* = 11.0, 1.1 Hz, 1H, H-28a), 3.84 (d, *J* = 11.0 Hz, 1H, H-28b), 3.06 (d, *J* = 14.4 Hz, 1H, H-30a), 2.90 (d, *J* = 14.4 Hz, 1H, H-30b), 2.54 – 2.43 (m, 4H), 2.39 – 2.32 (m, 1H, H-19), 2.06 (s, 3H, CH_3C=O), 2.04 (s, 3H, CH_3C=O), 1.03 (s, 3H, CH_3), 0.97 (s, 3H, CH_3), 0.86 – 0.84 (m, 6H, 2 × CH_3), 0.83 (s, 3H, CH_3). ^{13}C NMR (126 MHz, $CDCl_3$): δ 171.8 (-C=O, ester), 171.1 (-C=O, ester), 152.3 (C-20), 109.1 (C-29), 81.1 (C-3), 61.1 (-**C**H_2-OAc), 55.5, 54.7, 50.4, 49.6, 46.5, 44.9, 42.8, 41.1, 38.6, 37.9, 37.6, 37.2, 34.6, 34.3, 31.6, 29.9, 28.1, 27.2, 26.7, 23.8, 23.7, 21.5, 21.2, 21.1, 18.3, 16.6, 16.3, 16.2, 14.9. IR (DRIFT): 2941.65, 2868.40, 2784.49, 1733.25, 1460.32, 1364.05, 1239.48, 1029.25. HRMS (ASAP, TOF ES$^+$): calcd. for $C_{38}H_{62}NO_4^+$ $[M + H]^+$ 596.4673, found 596.4680.

*4.1.7.2. 3β,28-diacetoxy-30-(piperidin-1-yl)lup-20(29)-ene (**7b**).* Compound (**7b**) was prepared according to the general procedure for Tsuji-Trost reaction. The reaction time was 24 h. After the column chromatography purification using hexane/EtOAc (3:2) derivative **7b** was obtained in 71% yield as a white solid. R_f = 0.50 (hexane/EtOAc 3:2). $[\alpha]_D^{26}$ = −0.1 (c = 1.0, THF). ^{1}H NMR (500 MHz, $CDCl_3$): δ 4.88 – 4.80 (m, 2H, H-29), 4.50 – 4.43 (m, 1H, H-3), 4.25 (d, *J* = 11.0 Hz, 1H, H-28a), 3.84 (d, *J* = 11.0 Hz, 1H, H-28b), 2.82 (d, *J* = 14.2 Hz, 1H, H-30a), 2.74 (d, *J* = 14.2 Hz, 1H, H-30b), 2.50 – 2.20 (m, 5H, H-19, 2 × CH_2), 2.06 (s, 3H, CH_3C=O), 2.03 (s, 3H, CH_3C=O), 1.03 (s, 3H, CH_3), 0.97 (s, 3H, CH_3), 0.86 – 0.84 (m, 6H, 2 × CH_3), 0.83 (s, 3H, CH_3). ^{13}C NMR (126 MHz, $CDCl_3$): δ 171.8 (-C=O, ester), 171.1 (-C=O, ester), 151.5 (C-20), 109.8 (C-29), 81.1 (C-3), 64.3, 63.0 (-**C**H_2-OAc), 55.5, 55.2, 50.5, 49.6, 46.4, 44.8, 42.8, 41.1, 38.6, 37.9, 37.7, 37.2, 34.6, 34.3, 31.5, 30.0, 28.1, 27.2, 26.6, 26.2, 24.7, 23.8, 21.5, 21.2, 21.1, 18.3, 16.6, 16.3, 16.2, 14.9. IR (DRIFT): 2932.53, 2870.45, 1733.13, 1455.31, 1364.16, 1237.88, 1110.33, 1028.60. HRMS (ASAP, TOF ES$^+$): calcd. for $C_{39}H_{64}NO_4^+$ $[M + H]^+$ 610.4830, found 610.4833. The analytical data obtained in this study were compared with those reported in previously published research [41].

*4.1.7.3. 3β,28-diacetoxy-30-(morpholin-4-yl)lup-20(29)-ene (**7c**).* Compound (**7c**) was prepared according to the general procedure for Tsuji-Trost reaction. The reaction time was 24 h. After the column chromatography purification using a gradient mobile phase of hexane/EtOAc (6:1 to 4:1) derivative **7c** was obtained in 91% yield as a white solid. R_f = 0.37 (hexane/EtOAc 4:1). $[\alpha]_D^{25}$ = +12.8 (c = 1.0, THF). ^{1}H NMR (500 MHz, $CDCl_3$): δ 4.89 (d, *J* = 1.3 Hz, 1H, H-29), 4.87 (d, *J* = 1.1 Hz, 1H, H-29), 4.49 – 4.44 (m, 1H, H-3), 4.24 (dd, *J* = 11.1, 1.2 Hz, 1H, H-28a), 3.84 (d, *J* = 11.0 Hz, 1H, H-28b), 3.69 (t, *J* = 4.6 Hz, 4H, 2 × CH_2), 2.88 (d, *J* = 13.9 Hz, 1H, C-30a), 2.80 (d, *J* = 13.9 Hz, 1H, C-30b), 2.50 – 2.33 (m, 5H, H-19, 2 × CH_2), 2.07 (s, 3H, CH_3C=O), 2.04 (s, 3H, CH_3C=O), 1.03 (s, 3H, CH_3), 0.97 (s, 3H, CH_3), 0.85 (s, 3H, CH_3), 0.84 (s, 3H, CH_3), 0.83 (s, 3H, CH_3). ^{13}C NMR (126 MHz, $CDCl_3$): δ 171.8 (-C=O, ester), 171.1 (-C=O, ester), 150.6 (C-20), 110.5 (C-29), 81.1 (C-3), 67.3, 64.2, 62.9 (-**C**H_2-OAc), 55.5, 54.2, 50.5, 49.8, 46.4, 44.7, 42.8, 41.1, 38.6, 38.0, 37.7, 37.2, 34.6, 34.3, 31.7, 30.0, 28.1, 27.2, 26.8, 23.8, 21.5, 21.2, 21.1, 18.3, 16.6, 16.3, 16.2, 14.9. IR (DRIFT): 2940.91, 2870.45, 2800.86, 1732.38, 1454.18, 1364.55, 1238.91, 1117.22, 1029.55. HRMS (ASAP, TOF ES$^+$): calcd. for $C_{38}H_{62}NO_5^+$ $[M + H]^+$ 612.4623, found 612.4634. The analytical data obtained in this study were compared with those reported in previously published research [41].

*4.1.7.4. 3β,28-diacetoxy-30-(4-methylpiperazin-1-yl)lup-20(29)-ene (**7d**).* Compound (**7d**) was prepared according to the general procedure for Tsuji-Trost reaction. The reaction time was 24 h. After the column chromatography purification using EtOAc/MeOH (4:1) derivative **7d** was obtained in 75% yield as a white solid. R_f = 0.28 (EtOAc/MeOH 5:1). $[\alpha]_D^{25}$ = −3.4 (c = 1.0, THF). ^{1}H NMR (400 MHz, $CDCl_3$): δ 4.87 (d, *J* = 1.4 Hz, 1H, H-29), 4.85 (d, *J* = 1.4 Hz, 1H, H-29), 4.51 – 4.41 (m, 1H, H-3), 4.24 (dd, *J* = 11.1, 1.0 Hz, 1H, H-28a), 3.83 (d, *J* = 11.1 Hz, 1H, H-28b), 2.88 (d, *J* = 14.0 Hz, 1H, H-30a), 2.80 (d, *J* = 14.0 Hz, 1H, H-30b), 2.62 – 2.31 (m, 9H, H-19, 4 × CH_2), 2.28 (s, 3H, N-CH_3), 2.06 (s, 3H, CH_3C=O), 2.03 (s, 3H, CH_3C=O), 1.03 (s, 3H, CH_3), 0.97 (s, 3H, CH_3), 0.85 – 0.84 (m, 6H, 2 × CH_3), 0.83 (s, 3H, CH_3). ^{13}C NMR (101 MHz, $CDCl_3$): δ 171.8 (-C=O, ester), 171.1 (-C=O, ester), 151.0 (C-20), 110.2 (C-29), 81.1 (C-3), 62.9 (-**C**H_2-OAc), 55.5, 55.4, 53.7, 50.4, 49.7, 46.4, 46.2, 44.8, 42.8, 41.1, 38.6, 37.9, 37.7, 37.2, 34.6, 34.3, 31.6, 30.0, 29.8, 28.1, 27.2, 26.7, 23.8, 21.5, 21.2, 21.1, 18.3, 16.6, 16.3, 16.2, 15.0. IR (DRIFT): 2939.67, 2868.40, 2790.63, 1732.90, 1455.50, 1364.58, 1238.79, 1162.40, 1028.63, 1014.04. HRMS (ASAP, TOF ES$^+$): calcd. for $C_{39}H_{65}N_2O_4^+$ $[M + H]^+$ 625.4939, found 625.4946. The analytical data obtained in this study were compared with those reported in previously published research [41].

*4.1.7.5. 3β,28-diacetoxy-30-[4-(tert-butoxycarbonyl)piperazin-1-yl]lup-20(29)-ene (**7e**).* Compound (**7e**) was prepared according to the general procedure for Tsuji-Trost reaction. The reaction time was 24 h. After the column chromatography purification using hexane/EtOAc (6:1) derivative **7e** was obtained in 83% yield as a white solid. R_f = 0.26 (hexane/EtOAc 6:1). $[\alpha]_D^{25}$ = +1.1 (c = 1.0, THF). ^{1}H NMR (400 MHz, $CDCl_3$): δ 4.89 (d, *J* = 1.1 Hz, 1H, H-29), 4.86 (d, *J* = 1.0 Hz, 1H, H-29), 4.50 – 4.43 (m, 1H, H-3), 4.24 (d, *J* = 10.9 Hz, 1H, H-28a), 3.83 (d, *J* = 11.1 Hz,

1H, H-28b), 3.40 (t, $J = 5.0$ Hz, 4H, 2 × CH_2), 2.88 (d, $J = 13.9$ Hz, 1H, H-30a), 2.80 (d, $J = 13.9$ Hz, 1H, H-30b), 2.41 – 2.31 (m, 5H, H-19, 4 × CH_2), 2.07 (s, 3H, CH_3C=O), 2.04 (s, 3H, CH_3C=O), 1.46 (s, 9H, 3 × CH_3), 1.03 (s, 3H, CH_3), 0.97 (s, 3H, CH_3), 0.84 (s, 6H, 2 × CH_3), 0.83 (s, 3H, CH_3). ^{13}C NMR (101 MHz, $CDCl_3$): δ 171.8 (-C=O, ester), 171.1 (-C=O, ester), 155.0 (-C=O, carbamate), 150.9 (C-20), 110.5 (C-29), 81.0 (C-3), 79.6, 77.4, 62.9 (-**C**H_2-OAc), 55.5, 53.5, 50.4, 49.8, 46.4, 42.8, 41.1, 38.6, 38.0, 37.6, 37.2, 34.6, 34.3, 31.6, 30.0, 29.8, 28.6, 28.1, 27.2, 26.8, 23.8, 21.5, 21.2, 21.1, 18.3, 16.6, 16.3, 16.2, 14.9. IR (DRIFT): 2940.03, 2872.49, 1734.75, 1697.77, 1456.23, 1364.15, 1238.56, 1170.02, 1118.53, 1029.32, 1006.18. HRMS (ASAP, TOF ES$^+$): calcd. for $C_{43}H_{71}N_2O_6^+$ $[M + H]^+$ 711.5307, found 711.5306.

4.2. Biological evaluation

4.2.1. Cell culture and MTS cytotoxicity assay

The antiproliferative effects of the tested compounds were evaluated using a cytotoxicity screening workflow that has been routinely optimized and validated in our laboratory [74]. Unless stated otherwise, all cell lines were purchased from the American Type Culture Collection (ATCC). The CCRF-CEM human T-lymphoblastic leukemia cell line was employed as a highly chemosensitive model for hematological malignancies. The chronic myeloid leukemia cell line K562 harbors the BCR-ABL fusion oncogene and represents a model of Philadelphia chromosome-positive leukemia. U2OS cells, derived from human osteosarcoma, and A549 lung adenocarcinoma cells were used as representative solid tumor models. Colorectal carcinoma HCT116 cells and their isogenic p53-deficient derivative HCT116p53−/− (Horizon Discovery Ltd., UK) were included to assess the impact of p53 status on drug sensitivity. Human BJ foreskin fibroblasts and MRC-5 lung fibroblasts served as non-malignant control cell lines. Cells were maintained in cell culture flasks (75 cm^2) under standard conditions using Dulbecco's modified Eagle medium (DMEM) or RPMI-1640, as appropriate for each cell line, supplemented with 10% fetal calf serum, 2 mM L-glutamine, 5 g/L glucose, 100 U/mL penicillin, 100 μg/mL streptomycin, and sodium bicarbonate. Cultures were incubated at 37 °C in a humidified atmosphere containing 5% CO_2.

Cell viability and cytotoxicity were assessed using the MTS assay according to established procedures. Experiments were performed in three independent biological replicates, each conducted in technical triplicates. Cell viability was quantified spectrophotometrically following incubation with the MTS reagent and expressed relative to untreated controls, which were set to 100% viability.

4.2.2. Analysis of apoptotic Cell death by Annexin V/propidium iodide staining

Apoptotic cell death was evaluated using a flow-cytometric assay based on Annexin V-FITC and propidium iodide (PI) staining. Measurements were performed with a commercially available apoptosis detection kit (Exbio, Czech Republic), following the manufacturer's instructions with minor adaptations optimized for the CCRF-CEM cell line. Cells were harvested, adjusted to the appropriate density, and washed with Annexin V binding buffer prior to staining. Cells were subsequently incubated with Annexin V-FITC and propidium iodide, however, to minimize nonspecific cytotoxic effects observed in CCRF-CEM cells, the amount of propidium iodide was reduced to 50% of the recommended concentration, as the standard protocol resulted in acute membrane damage. After staining, samples were incubated for 15 min at room temperature in the dark, centrifuged, and resuspended in 100 μL of Annexin V binding buffer. Flow-cytometric analysis was performed immediately using a FACSAria II cytometer (Becton Dickinson). For each sample, at least 10 000 events corresponding to intact cells were acquired and analyzed. Data were evaluated to distinguish viable, early apoptotic, late apoptotic, and necrotic cell populations based on Annexin V and PI fluorescence characteristics.

4.2.3. Assessment of mitochondrial membrane potential using JC-1 dye

Alterations in mitochondrial membrane potential (ΔΨm) were examined by flow cytometry using the potential-sensitive cationic dye JC-1. CCRF-CEM cells were treated with the indicated compounds at concentrations corresponding to 1× and 5 × IC_{50} for 6 h. This shortened treatment interval was selected to allow reliable assessment of mitochondrial function prior to extensive loss of cellular integrity observed at longer exposure times. Following treatment, cells were collected and adjusted to a density of 0.5×10^6 cells/mL, then incubated with JC-1 at a final concentration of 1 μM for 10 min at room temperature. To verify assay performance and provide a reference for complete mitochondrial depolarization, cells were treated with the protonophore carbonyl cyanide m-chlorophenyl hydrazone (CCCP, 100 μM) for 5 min prior to JC-1 staining. After incubation, cells were pelleted by centrifugation (1500 rpm, 5 min, room temperature), resuspended in 0.5 mL of phosphate-buffered saline, and immediately subjected to flow-cytometric analysis. Data acquisition was performed using a FACSAria II flow cytometer (Becton Dickinson) equipped with a 488 nm excitation laser. Emission from JC-1 monomers and aggregates, corresponding to depolarized and polarized mitochondria, respectively, was detected using appropriate fluorescence channels centered at 529 nm (green) and 590 nm (red). Forward- and side-scatter parameters were used to gate intact cells and exclude cellular debris prior to ΔΨm analysis. For each condition, a minimum of 10 000 events within the defined gate were recorded and evaluated.

4.2.4. Flow-cytometric analysis of cell-cycle distribution and mitotic activity

Cell-cycle progression was analyzed by flow cytometry based on total DNA content determination following propidium iodide (PI) staining. CCRF-CEM cells were seeded at a density of 5×10^5 cells/mL in 6-well culture plates and treated with the tested compounds at concentrations corresponding to 1× or 5 × IC_{50} for 24 h. Cells were cultured in RPMI 1640 medium supplemented with 10% fetal calf serum, 100 U/mL penicillin, and 100 μg/mL streptomycin under standard incubation conditions (37 °C, 5% CO_2). Vehicle-treated cells were included as parallel controls. Following treatment, cells were harvested, washed with ice-cold phosphate buffered saline (PBS), and fixed in 70% ethanol at −20 °C overnight. Fixed samples were subsequently washed in hypotonic citrate buffer, treated with RNase A (50 μg/mL), and stained with propidium iodide for DNA content analysis. Flow-cytometric acquisition was performed using a FACSCalibur cytometer (Becton Dickinson) equipped with a 488 nm excitation laser. Cell-cycle phase distribution (G1, S, and G2/M) was quantified using Kaluza software (Beckman Coulter).

Mitotic activity was assessed in parallel by immunofluorescent detection of histone H3 phosphorylated at serine 10 (pH3Ser10). An aliquot of each sample was stained with an anti-pH3Ser10 antibody (Sigma-Aldrich) according to established protocols and analyzed by flow cytometry to determine the proportion of mitotic cells, as previously described in [74].

4.2.5. Evaluation of DNA synthesis by BrdU incorporation

DNA replication activity was assessed under experimental conditions identical to those used for cell-cycle analysis. Following compound treatment, CCRF-CEM cells were pulse-labeled with 5-bromo-2′-deoxyuridine (BrdU) at a final concentration of 10 μM for 30 min prior to harvesting to detect newly synthesized DNA. Cells were then collected by trypsinization, washed, and fixed in ice-cold 70% ethanol for 30 min on ice. After fixation, cells were washed with phosphate buffered saline (PBS) and subjected to DNA denaturation by incubation in 2 M hydrochloric acid for 30 min at room temperature to allow antibody access to incorporated BrdU. The reaction was subsequently neutralized using 0.1 M sodium tetraborate ($Na_2B_4O_7$), followed by washing in PBS supplemented with 0.5% Tween-20 and 1% bovine serum albumin to reduce nonspecific binding. BrdU incorporation was detected by

incubation with a primary anti-BrdU antibody (Exbio, Czech Republic) for 30 min at room temperature in the dark. After washing, cells were stained with a fluorescein-conjugated secondary anti-mouse antibody (Sigma-Aldrich). Prior to analysis, cells were counterstained with propidium iodide (0.1 mg/mL) and treated with RNase A (0.5 mg/mL) for 1 h at room temperature in the dark. Flow-cytometric measurements were performed using a FACSCalibur cytometer (Becton Dickinson) equipped with a 488 nm excitation laser. Intact cells were selected based on forward- and side-scatter parameters before evaluation of BrdU incorporation.

4.2.6. *Evaluation of RNA synthesis by BrU incorporation*

RNA synthesis was analyzed under experimental conditions identical to those used for cell-cycle analysis. Following compound treatment, CCRF-CEM cells were pulse-labeled with 5-bromouridine (BrU) at a final concentration of 1 mM for 30 min prior to harvesting in order to mark newly synthesized RNA. After labeling, cells were fixed in phosphate-buffered saline containing 1% paraformaldehyde and 0.05% NP-40 for 15 min at room temperature. To enhance fixation efficiency, samples were subsequently incubated at 4 °C overnight. Residual aldehyde groups were quenched by incubation with 1% glycine in PBS, followed by thorough washing steps. Incorporated BrU was detected by immunofluorescence using a primary anti-BrdU antibody (Exbio, Czech Republic), which is cross-reactive with BrU, and a fluorescein-conjugated secondary anti-mouse antibody (Sigma-Aldrich). Both antibody incubations were performed for 30 min at room temperature in the dark. To stabilize fluorescence signals, cells were subjected to a second fixation step in 1% paraformaldehyde containing 0.05% NP-40. Prior to flow-cytometric acquisition, cells were counterstained with propidium iodide (0.1 mg/mL) and treated with RNase A (0.5 mg/mL) for 1 h at room temperature in the dark. Analysis was performed using a FACSCalibur flow cytometer (Becton Dickinson) equipped with a 488 nm excitation laser. Intact cells were selected based on forward- and side-scatter parameters before evaluation of BrU incorporation.

4.2.7. *Western blot analysis*

For protein expression analysis, CCRF-CEM cells were treated with the selected compounds at concentrations corresponding to 1 × IC_{50} for 24 h. After treatment, cells were collected, washed thoroughly with ice-cold phosphate-buffered saline (PBS), and lysed in RIPA buffer (50 mM Tris-HCl, pH 8.0; 150 mM NaCl; 1% NP-40; 0.5% sodium deoxycholate; 0.1% SDS; 1 mM EDTA) supplemented with cOmplete™ protease and phosphatase inhibitor cocktails (Roche). Total protein concentration in cell lysates was determined using the Pierce™ BCA Protein Assay Kit (Thermo Scientific) according to the manufacturer's instructions. Equal amounts of protein (20 μg per lane) were mixed with Laemmli sample buffer, denatured, and subsequently separated by SDS-polyacrylamide gel electrophoresis (SDS-PAGE). Proteins were then transferred onto nitrocellulose membranes using the Trans-Blot® Turbo™ Transfer System (Bio-Rad). Following transfer, membranes were blocked in 5% bovine serum albumin (BSA) prepared in Tris-buffered saline containing 0.1% Tween-20 (TBS-T) for 1 h at room temperature. Blots were incubated overnight at 4 °C with primary antibodies directed against proteins involved in DNA damage response, cell-cycle regulation, and apoptosis, including γH2AX (Novus Biologicals); PCNA, Chk1, Cyclin E1, and p21 (Santa Cruz Biotechnology); β-actin (Sigma-Aldrich); and PARP, caspase-3, BAX, and Bcl-xL (Cell Signaling Technology). After incubation, membranes were washed with TBS-T and probed with appropriate horseradish peroxidase (HRP)-conjugated secondary antibodies for 1 h at room temperature. Protein bands were detected using ECL Prime chemiluminescent substrate (Amersham) and visualized with the LI-COR Odyssey imaging system (LI-COR Biotechnology). β-Actin was used as a loading control to confirm equal protein loading across samples.

CRediT authorship contribution statement

Jan Bachořík: Conceptualization, Data curation, Investigation, Methodology, Validation, Writing – original draft. **Ivo Frydrych:** Conceptualization, Data curation, Formal analysis, Investigation, Methodology, Writing – original draft, Writing – review & editing. **Soňa Gurská:** Data curation, Formal analysis, Validation. **Štěpán Dostál:** Data curation, Formal analysis, Investigation. **Jan Pokorný:** Formal analysis, Writing – original draft. **Adam Přibylka:** Data curation, Formal analysis. **Martina Medvedíková:** Data curation, Formal analysis. **Petr Džubák:** Formal analysis, Supervision, Validation, Writing – review & editing. **Marián Hajdúch:** Funding acquisition, Supervision. **Milan Urban:** Conceptualization, Data curation, Formal analysis, Funding acquisition, Project administration, Resources, Supervision, Validation, Writing – original draft, Writing – review & editing.

Declaration of competing interest

The authors declare that they have no known competing financial interests or personal relationships that could have appeared to influence the work reported in this paper.

Acknowledgment

This work was supported by the SALVAGE project, registration number: CZ.02.01.01/00/22_008/0004644, supported by OP JAK, with co-financing from the EU and the State Budget. The infrastructure was supported in parts by the infrastructural projects (CZ-OPENSCREEN – LM2023052; EATRIS-CZ – LM2023053). Pharmacology studies and stipends for students were supported by internal Palacký University grants IGA_LF_2025_021 and IGA_PrF_2026_015.

Appendix A. Supplementary data

Supplementary data to this article can be found online at https://doi.org/10.1016/j.ejmcr.2026.100360.

Data availability

Data will be made available on request.

References

[1] H. El Allaoui, K. El Ahmadi, A. El Abdouni, I. Dira, M. El Bastrioui, M. Bouhrim, B. Eto, A.A. Shahat, R.N. Herqash, K. Haboubi, Trends and insights in medicinal plant extract research: a ten-year bibliometric and visualization study, Horticulturae 10 (2024) 1163, https://doi.org/10.3390/horticulturae10111163.
[2] M.M. O'Connell, M.D. Bentley, C.S. Campbell, B.J.W. Cole, Betulin and lupeol in bark from four white-barked birches, Phytochemistry 27 (1988) 2175–2176, https://doi.org/10.1016/0031-9422(88)80120-1.
[3] G. Zhao, W. Yan, D. Cao, Simultaneous determination of betulin and betulinic acid in white birch bark using RP-HPLC, J. Pharmaceut. Biomed. Anal. 43 (2007) 959–962, https://doi.org/10.1016/j.jpba.2006.09.026.
[4] Z. Yu-hong, Y. Tao, W. Yang, Extraction of betulin from bark ofBetula platyphylla by supercritical carbon dioxide extraction, J. For. Res. 14 (2003) 202–204, https://doi.org/10.1007/BF02856830.
[5] A.Z. Abyshev, É.M. Agaev, A.B. Guseinov, Studies of the chemical composition of birch bark extracts (Cortex betula) from the Betulaceae family, Pharm. Chem. J. 41 (2007) 419–423, https://doi.org/10.1007/s11094-007-0091-5.
[6] A. Fălămaş, S.C. Pînzaru, C.A. Dehelean, C.I. Peev, C. Soica, Betulin and its natural resource as potential anticancer drug candidate seen by FT-Raman and FT-IR spectroscopy, J. Raman Spectrosc. 42 (2011) 97–107, https://doi.org/10.1002/jrs.2658.
[7] L. Holonec, F. Ranga, D. Crainic, A. Truta, C. Socaciu, Evaluation of Betulin and betulinic acid content in birch bark from different forestry areas of Western carpathians, Not Bot Horti Agrobo 40 (2012) 99–105, https://doi.org/10.15835/nbha4027967.
[8] S.K. Król, M. Kiełbus, A. Rivero-Müller, A. Stepulak, Comprehensive review on betulin as a potent anticancer agent, BioMed Res. Int. 2015 (2015) 584189, https://doi.org/10.1155/2015/584189.
[9] J. Cabaj, W. Bąk, P. Wróblewska-Łuczka, Anti-cancer effect of betulin and its derivatives, with particular emphasis on the treatment of melanoma, J Pre Clin Clin Res. 15 (2021) 73–79, https://doi.org/10.26444/jpccr/135691.

[10] H.S. Tuli, K. Sak, D.S. Gupta, G. Kaur, D. Aggarwal, N.C. Parashar, R. Choudhary, M.B. Yerer, J. Kaur, M. Kumar, V.K. Garg, G. Sethi, Anti-inflammatory and anticancer properties of Birch bark-derived betulin: recent developments, Plants 10 (2021), https://doi.org/10.3390/plants10122663.
[11] E. Nemli, B. Saricaoglu, C. Kirkin, G. Ozkan, E. Capanoglu, S. Habtemariam, J. Sharifi-Rad, D. Calina, Chemopreventive and chemotherapeutic potential of betulin and betulinic acid: mechanistic insights from in vitro, in vivo and clinical studies, Food Sci. Nutr. 12 (2024) 10059–10069, https://doi.org/10.1002/fsn3.4639.
[12] W. Rzeski, A. Stepulak, M. Szymański, M. Juszczak, A. Grabarska, M. Sifringer, J. Kaczor, M. Kandefer-Szerszeń, Betulin elicits anti-cancer effects in tumour primary cultures and cell lines in vitro, Basic Clin. Pharmacol. Toxicol. 105 (2009) 425–432, https://doi.org/10.1111/j.1742-7843.2009.00471.x.
[13] E.M. Terefe, F.A. Okalebo, S. Derese, M.K. Langat, E. Mas-Claret, N.H. Aljarba, S. Alkahtani, G.E.-S. Batiha, A. Ghosh, E.A. El-Masry, J. Muriuki, In vitro anti-HIV and cytotoxic effects of pure compounds isolated from Croton macrostachyus Hochst. Ex Delile, BMC Complement. Med. Ther. 22 (2022) 159, https://doi.org/10.1186/s12906-022-03638-6.
[14] I.-C. Sun, J.-K. Shen, H.-K. Wang, L.M. Cosentino, K.-H. Lee, Anti-AIDS agents. 32.1 synthesis and anti-HIV activity of betulin derivatives, Bioorg. Med. Chem. Lett 8 (1998) 1267–1272, https://doi.org/10.1016/S0960-894X(98)00202-9.
[15] W. Szlasa, S. Ślusarczyk, I. Nawrot-Hadzik, R. Abel, A. Zalesińska, A. Szewczyk, N. Sauer, R. Preissner, J. Saczko, M. Drąg, M. Poręba, M. Daczewska, J. Kulbacka, M. Drąg-Zalesińska, Betulin and its derivatives reduce inflammation and COX-2 activity in macrophages, Inflammation 46 (2023) 573–583, https://doi.org/10.1007/s10753-022-01756-4.
[16] C. Kruszniewska-Rajs, B. Strzałka-Mrozik, M. Kimsa-Dudek, A. Synowiec-Wojtarowicz, E. Chrobak, E. Bębenek, S. Boryczka, S. Głuszek, J.M. Gola, The influence of betulin and its derivatives EB5 and ECH147 on the antioxidant status of human renal proximal tubule epithelial cells, Int. J. Mol. Sci. 23 (2022) 2524, https://doi.org/10.3390/ijms23052524.
[17] G. Xia, C. Shen, Y. Xiao, X. Wang, L. Qiu, S. Lei, R. Jiang, Shenling Baizhu Powder and Betulin attenuate sepsis-induced intestinal injury by targeting GADD45B/TAOK1/p38 MAPK pathway, J. Ethnopharmacol. 353 (2025) 120282, https://doi.org/10.1016/j.jep.2025.120282.
[18] S. Jäger, M.N. Laszczyk, A. Scheffler, A preliminary pharmacokinetic Study of betulin, the main pentacyclic triterpene from extract of outer bark of birch (Betulae alba cortex), Molecules 13 (2008) 3224–3235, https://doi.org/10.3390/molecules13123224.
[19] L. Zhang, J. Song, L. Kong, T. Yuan, W. Li, W. Zhang, B. Hou, Y. Lu, G. Du, The strategies and techniques of drug discovery from natural products, Pharmacol. Therapeut. 216 (2020) 107686, https://doi.org/10.1016/j.pharmthera.2020.107686.
[20] E. Chrobak, M. Świtalska, J. Wietrzyk, E. Bębenek, New difunctional derivatives of betulin: preparation, characterization and antiproliferative potential, Molecules 30 (2025) 611, https://doi.org/10.3390/molecules30030611.
[21] R. Csuk, A. Barthel, R. Kluge, D. Ströhl, Synthesis, cytotoxicity and liposome preparation of 28-acetylenic betulin derivatives, Bioorg. Med. Chem. 18 (2010) 7252–7259, https://doi.org/10.1016/j.bmc.2010.08.023.
[22] S. Boryczka, E. Bębenek, J. Wietrzyk, K. Kempińska, M. Jastrzębska, J. Kusz, M. Nowak, Synthesis, structure and cytotoxic activity of new acetylenic derivatives of betulin, Molecules 18 (2013) 4526–4543, https://doi.org/10.3390/molecules18044526.
[23] R. Csuk, A. Barthel, R. Sczepek, B. Siewert, S. Schwarz, Synthesis, encapsulation and antitumor activity of new betulin derivatives, Arch. Pharmazie 344 (2011) 37–49, https://doi.org/10.1002/ardp.201000232.
[24] L. Heller, V. Perl, J. Wiemann, A. Al-Harrasi, R. Csuk, Amino(oxo)acetate moiety: a new functional group to improve the cytotoxicity of betulin derived carbamates, Bioorg Med Chem Lett 26 (2016) 2852–2854, https://doi.org/10.1016/j.bmcl.2016.04.055.
[25] O.V. Tsepaeva, A.V. Nemtarev, T.I. Abdullin, L.R. Grigor'eva, E.V. Kuznetsova, R. A. Akhmadishina, L.E. Ziganshina, H.H. Cong, V.F. Mironov, Design, synthesis, and cancer cell growth inhibitory activity of triphenylphosphonium derivatives of the Triterpenoid betulin, J. Nat. Prod. 80 (2017) 2232–2239, https://doi.org/10.1021/acs.jnatprod.7b00105.
[26] O.B. Kazakova, I.E. Smirnova, L.A. Baltina, E.I. Boreko, O.V. Savinova, A. G. Pokrovskii, Antiviral activity of acyl derivatives of betulin and betulinic and dihydroquinopimaric acids, Russ. J. Bioorg. Chem. 44 (2018) 740–744, https://doi.org/10.1134/S1068162018050059.
[27] M. Grymel, G. Pastuch-Gawołek, A. Lalik, M. Zawojak, S. Boczek, M. Krawczyk, K. Erfurt, Glycoconjugation of betulin derivatives using copper-catalyzed 1,3-Dipolar azido-alkyne cycloaddition reaction and a preliminary assay of cytotoxicity of the obtained compounds, Molecules 25 (2020) 6019, https://doi.org/10.3390/molecules25246019.
[28] A. Aye Mar, A. Koohang, N.D. Majewski, E.L. Szotek, D.A. Eiznhamer, M.T. Flavin, Z.Q. Xu, Synthesis and cytotoxicity of 28-carboxymethoxy lupane triterpenoids. Preference of 28-*O*-acylation over 28-*O*-alkylation of betulin by ethyl bromoacetate, Chin. Chem. Lett. 20 (2009) 1141–1144, https://doi.org/10.1016/j.cclet.2009.04.001.
[29] Y. Kashiwada, J. Chiyo, Y. Ikeshiro, T. Nagao, H. Okabe, L.M. Cosentino, K. Fowke, K.H. Lee, 3,28-Di-O-(dimethylsuccinyl)-betulin isomers as anti-HIV agents1, Bioorg. Med. Chem. Lett 11 (2001) 183–185, https://doi.org/10.1016/S0960-894X(00)00635-1.
[30] R.C. Santos, J.A.R. Salvador, S. Marín, M. Cascante, Novel semisynthetic derivatives of betulin and betulinic acid with cytotoxic activity, Bioorg. Med. Chem. 17 (2009) 6241–6250, https://doi.org/10.1016/j.bmc.2009.07.050.
[31] V.A. Levdanskii, A.V. Levdanskii, B.N. Kuznetsov, Sulfation of betulin by sulfamic acid in DMF and dioxane, Chem. Nat. Compd. 50 (2014) 1029–1031, https://doi.org/10.1007/s10600-014-1152-0.
[32] E. Bębenek, M. Kadela-Tomanek, E. Chrobak, J. Wietrzyk, J. Sadowska, S. Boryczka, New acetylenic derivatives of betulin and betulone, synthesis and cytotoxic activity, Med. Chem. Res. 26 (2017) 1–8, https://doi.org/10.1007/s00044-016-1713-9.
[33] Y.B. Zhang, S.W. Pan, M. Zhang, X.S. Guo, J.F. Wang, M. Bu, Design and synthesis of novel betulin derivatives containing thiazole moiety as anticancer agents, Russ. J. Gen. Chem. 95 (2025) 679–689, https://doi.org/10.1134/S1070363224613206.
[34] M. Kadela-Tomanek, E. Chrobak, E. Bębenek, 28-[1-(3-(Propionyloxy)propyl)-1H-1,2,3-triazol-4-yl]carbonylbetulin, Molbank 2022. https://doi.org/10.3390/M1487, 2022.
[35] V.A. Levdanskii, A.V. Levdanskii, B.N. Kuznetsov, Synthesis of Betulin dibenzoate and diphthalate, Chem. Nat. Compd. 53 (2017) 310–311, https://doi.org/10.1007/s10600-017-1976-5.
[36] A.V. Levdansky, N.V. Garyntseva, V.A. Levdansky, Esterification of Betulin 3-Acetate in melts of some organic acids, Chem. Nat. Compd. 59 (2023) 862–864, https://doi.org/10.1007/s10600-023-04136-y.
[37] E. Chrobak, E. Bębenek, K. Marciniec, M. Kadela-Tomanek, S. Siudak, M. Latocha, S. Boryczka, New 30-substituted derivatives of pentacyclic triterpenes: preparation, biological activity, and molecular docking study, J. Mol. Struct. 1226 (2021) 129394, https://doi.org/10.1016/j.molstruc.2020.129394.
[38] I.-C. Sun, H.-K. Wang, Y. Kashiwada, J.-K. Shen, L.M. Cosentino, C.-H. Chen, L.-M. Yang, K.-H. Lee, Anti-AIDS agents. 34. Synthesis and Structure−Activity relationships of betulin derivatives as Anti-HIV agents, J. Med. Chem. 41 (1998) 4648–4657, https://doi.org/10.1021/jm980391g.
[39] S. Pramanick, S. Mandal, S. Mukhopadhyay, S. Jha, Allylic hydroxylation through acid catalysed epoxy ring opening of betulinic acid derivatives, Synth. Commun. 35 (2005) 2143–2148, https://doi.org/10.1080/00397910500180568.
[40] A. Günther, E. Makuch, A. Nowak, W. Duchnik, Ł. Kucharski, R. Pełech, A. Klimowicz, Enhancement of the antioxidant and skin permeation properties of betulin and its derivatives, Molecules 26 (2021) 3435, https://doi.org/10.3390/molecules26113435.
[41] N.V. Uzenkova, N.I. Petrenko, M.M. Shakirov, E.E. Shul'ts, G.A. Tolstikov, Synthesis of 30-Amino derivatives of lupane triterpenoids, Chem. Nat. Compd. 41 (2005) 692–700, https://doi.org/10.1007/s10600-006-0014-9.
[42] O.B. Flekhter, I.E. Smirnova, F.Z. Galin, G.V. Giniyatullina, E.V. Tret'yakova, G. A. Tolstikov, Synthesis of 30-amino derivatives of 3,28-di-O-acetylbetulin, Chem. Nat. Compd. 40 (2004) 571–573, https://doi.org/10.1007/s10600-005-0039-5.
[43] G.R. Pettit, N. Melody, J.-C. Chapuis, Antineoplastic agents. 606. The betulastatins, J. Nat. Prod. 81 (2018) 458–464, https://doi.org/10.1021/acs.jnatprod.7b00536.
[44] A.A. Mar, E.L. Szotek, A. Koohang, W.P. Flavin, D.A. Eiznhamer, M.T. Flavin, Z.-Q. Xu, Synthesis, proapoptotic screening, and structure–activity relationships of novel aza-lupane triterpenoids, Bioorg. Med. Chem. Lett 20 (2010) 5389–5393, https://doi.org/10.1016/j.bmcl.2010.07.120.
[45] A.Yu Spivak, D.A. Nedopekina, R.R. Gubaidullin, E.V. Davletshin, A. A. Tukhbatullin, V.A. D'yakonov, M.M. Yunusbaeva, L.U. Dzhemileva, U. M. Dzhemilev, Pentacyclic triterpene acid conjugated with mitochondria-targeting cation F16: synthesis and evaluation of cytotoxic activities, Med. Chem. Res. 30 (2021) 940–951, https://doi.org/10.1007/s00044-021-02702-z.
[46] J. Pokorny, V. Horka, V. Sidova, M. Urban, Synthesis and characterization of new conjugates of betulin diacetate and bis(triphenysilyl)betulin with substituted triazoles, Monatsh. Chem. 149 (2018) 839–845, https://doi.org/10.1007/s00706-017-2113-7.
[47] W.F. Chi, L. Jin, F.-Y. Piao, R.-B. Han, Synthesis of betulin derivatives containing triazole fragments, Chem. Nat. Compd. 49 (2013) 264–267, https://doi.org/10.1007/s10600-013-0577-1.
[48] A.N. Antimonova, N.I. Petrenko, M.M. Shakirov, T.V. Rybalova, T.S. Frolova, E. E. Shul'ts, T.P. Kukina, O.I. Sinitsyna, G.A. Tolstikov, Synthesis and study of mutagenic properties of lupane triterpenoids containing 1,2,3-triazole fragments in the C-30 position, Chem. Nat. Compd. 49 (2013) 657–664, https://doi.org/10.1007/s10600-013-0702-1.
[49] V.A. Glushkov, D.A. Shemyakina, N.K. Zhukova, L.V. Pavlogradskaya, M. V. Dmitriev, D.V. Eroshenko, A.R. Galeev, I.G. Mokrushin, Ferrocenyltriazoles from 3β,28-Diacylbetulin: synthesis and cytotoxic activity, Russ. J. Org. Chem. 55 (2019) 1690–1697, https://doi.org/10.1134/S1070428019110083.
[50] G. Feng, T. Wang, R. Zhang, J. Luo, M. Xiao, H. Baoen, Y. Liu, J. Wu, New betulin nitrates: synthesis, cytotoxic activity and molecular docking evaluation, Acta Poloniae Pharmaceutica - Drug Research 75 (2018) 1135–1145, https://doi.org/10.32383/appdr/81731.
[51] I.A. Tolmacheva, L.N. Shelepen'kina, YuB. Vikharev, L.V. Anikina, V.V. Grishko, A. G. Tolstikov, Synthesis and biological activity of S-Containing betulin derivatives, Chem. Nat. Compd. 41 (2005) 701–705, https://doi.org/10.1007/s10600-006-0015-8.
[52] E. Chrobak, E. Bębenek, M. Kadela-Tomanek, M. Latocha, C. Jelsch, E. Wenger, S. Boryczka, Betulin phosphonates; synthesis, structure, and cytotoxic activity, Molecules 21 (2016) 1123, https://doi.org/10.3390/molecules21091123.
[53] F.-Y. Huang, B.Y. Chung, M.D. Bentley, A.R. Alford, Colorado potato beetle antifeedants by simple modification of the birch bark triterpene betulin, J. Agric. Food Chem. 43 (1995) 2513–2516, https://doi.org/10.1021/jf00057a035.
[54] S.D. Roughley, A.M. Jordan, The medicinal chemist's toolbox: an analysis of reactions used in the pursuit of drug candidates, J. Med. Chem. 54 (2011) 3451–3479, https://doi.org/10.1021/jm200187y.
[55] S.K. Rath, R.K. Nagar, S. Das, G. Yadav, D. Mukherjee, B. Singh, S. Singh, P. L. Sangwan, C-30 analogues of betulinic acid as potent cytotoxic agents: design,

synthesis, biological evaluation and in-silico studies, J. Biomol. Struct. Dyn. 43 (2025) 4564–4577, https://doi.org/10.1080/07391102.2024.2303612.
[56] F. Graziosi, J. Arduini, P. Bonasoni, F. Furlani, U. Giostra, A.J. Manning, A. McCulloch, S. O'Doherty, P.G. Simmonds, S. Reimann, M.K. Vollmer, M. Maione, Emissions of carbon tetrachloride from Europe, Atmos. Chem. Phys. 16 (2016) 12849–12859, https://doi.org/10.5194/acp-16-12849-2016.
[57] J. Bachořík, I. Frydrych, S. Gurská, Š. Dostál, J. Pokorný, P. Džubák, M. Hajdúch, M. Urban, New synthetic approach to C-30 ethers, esters, and amines of betulin using the Mitsunobu reaction and biological evaluation of the products, ACS Omega (2026), https://doi.org/10.1021/acsomega.6c00716.
[58] H. Kinoshita, H. Shinokubo, K. Oshima, Water enables direct use of Allyl alcohol for tsuji−trost reaction without activators, Org. Lett. 6 (2004) 4085–4088, https://doi.org/10.1021/ol048207a.
[59] O. Pàmies, J. Margalef, S. Cañellas, J. James, E. Judge, P.J. Guiry, C. Moberg, J.-E. Bäckvall, A. Pfaltz, M.A. Pericàs, M. Diéguez, Recent advances in enantioselective Pd-Catalyzed allylic substitution: from design to applications, Chem. Rev. 121 (2021) 4373–4505, https://doi.org/10.1021/acs.chemrev.0c00736.
[60] M. Evers, C. Poujade, F. Soler, Y. Ribeill, C. James, Y. Lelièvre, J.-C. Gueguen, D. Reisdorf, I. Morize, R. Pauwels, E. De Clercq, Y. Hénin, A. Bousseau, J.-F. Mayaux, J.-B. Le Pecq, N. Dereu, Betulinic acid derivatives: a new class of human immunodeficiency virus type 1 specific inhibitors with a new mode of action, J. Med. Chem. 39 (1996) 1056–1068, https://doi.org/10.1021/jm950670t.
[61] V. Sidova, P. Zoufaly, J. Pokorny, P. Dzubak, M. Hajduch, I. Popa, M. Urban, Cytotoxic conjugates of betulinic acid and substituted triazoles prepared by Huisgen Cycloaddition from 30-azidoderivatives, PLoS One 12 (2017) e0171621, https://doi.org/10.1371/journal.pone.0171621.
[62] M. Urban, J. Sarek, I. Tislerova, P. Dzubak, M. Hajduch, Influence of esterification and modification of A-ring in a group of lupane acids on their cytotoxicity, Bioorg. Med. Chem. 13 (2005) 5527–5535, https://doi.org/10.1016/j.bmc.2005.07.011.
[63] J. Hodoň, I. Frydrych, Z. Trhlíková, J. Pokorný, L. Borková, S. Benická, M. Vlk, B. Lišková, A. Kubíčková, M. Medvedíková, M. Pisár, J. Šarek, V. Das, A. Ligasová, K. Koberna, P. Džubák, M. Hajdúch, M. Urban, Triterpenoid pyrazines and pyridines – synthesis, cytotoxicity, mechanism of action, preparation of prodrugs, Eur. J. Med. Chem. 243 (2022) 114777, https://doi.org/10.1016/j.ejmech.2022.114777.
[64] A. Kazakova, I. Frydrych, N. Jakubcová, J. Pokorný, B. Lišková, S. Gurská, R. Buriánová, A. Přibylka, P. Džubák, M. Hajdúch, M. Urban, Triterpenoid phthalimides as selective anti-cancer agents targeting mitochondrial apoptosis, Eur. J. Med. Chem. 283 (2025) 117126, https://doi.org/10.1016/j.ejmech.2024.117126.
[65] A.F. Nassar, Structural modifications of drug candidates: how useful are they in improving metabolic stability of new drugs? Part I: enhancing metabolic stability, in: Drug Metabolism Handbook, John Wiley & Sons, Ltd, 2008, pp. 253–268, https://doi.org/10.1002/9780470439265.ch10.
[66] F. Wohnsland, B. Faller, High-throughput permeability pH profile and high-throughput Alkane/Water log *P* with artificial membranes, J. Med. Chem. 44 (2001) 923–930, https://doi.org/10.1021/jm001020e.
[67] P. Artursson, K. Palm, K. Luthman, Caco-2 monolayers in experimental and theoretical predictions of drug transport1PII of original article: S0169-409X(96)00415-2, The article was originally published in Advanced Drug Delivery Reviews 22 (1996) 67–84.1, Adv. Drug Deliv. Rev. 46 (2001) 27–43, https://doi.org/10.1016/S0169-409X(00)00128-9.
[68] J.D. Irvine, L. Takahashi, K. Lockhart, J. Cheong, J.W. Tolan, H.E. Selick, J. R. Grove, MDCK (Madin-Darby canine kidney) cells: a tool for membrane permeability screening, J. Pharmaceut. Sci. 88 (1999) 28–33, https://doi.org/10.1021/js9803205.
[69] P. Ghosh, A. Mandal, J. Ghosh, C. Pal, A.K. Nanda, Synthesis of bioactive 28-hydroxy-3-oxolup-20(29)-en-30-al with antileukemic activity, J. Asian Nat. Prod. Res. 14 (2012) 141–153, https://doi.org/10.1080/10286020.2011.640774.
[70] K. Komizo, H. Ikedo, S. Sato, S. Takenaka, Metallization of double-stranded DNA triggered by bound galactose-modified naphthalene diimide, Bioconjug. Chem. 25 (2014) 1547–1555, https://doi.org/10.1021/bc500263b.
[71] B. Doboszewski, E. Groaz, P. Herdewijn, Synthesis of phosphonoglycine backbone units for the development of Phosphono peptide nucleic acids, Eur. J. Org Chem. 2013 (2013) 4804–4815, https://doi.org/10.1002/ejoc.201300523.
[72] H. Ikeuchi, M.E. Meyer, Y. Ding, J. Hiratake, N.G.J. Richards, A critical electrostatic interaction mediates inhibitor recognition by human asparagine synthetase, Bioorg. Med. Chem. 17 (2009) 6641–6650, https://doi.org/10.1016/j.bmc.2009.07.071.
[73] T. Tamura, S. Nakano, E. Nakata, T. Morii, Construction of a library of structurally diverse ribonucleopeptides with catalytic groups, Bioorg. Med. Chem. 25 (2017) 1881–1888, https://doi.org/10.1016/j.bmc.2017.02.007.
[74] R. Kaplánek, M. Jakubek, J. Rak, Z. Kejík, M. Havlík, B. Dolenský, I. Frydrych, M. Hajdúch, M. Kolář, K. Bogdanová, J. Králová, P. Džubák, V. Král, Caffeine-hydrazones as anticancer agents with pronounced selectivity toward T-lymphoblastic leukaemia cells, Bioorg. Chem. 60 (2015) 19–29, https://doi.org/10.1016/j.bioorg.2015.03.003.